

CHAPTER 2 – CONCEPTS AND METHODOLOGY OF STRESS ANALYSIS

This Chapter focuses on the methodological and conceptual ideas that have been applied in this research. After a short introduction on stress in the Earth's crust, special attention will be paid to:

- 1) The paleostress (fault inversion) method, which has been used to determine the evolution of the stress field in the Iberian Peninsula through the Tertiary;
- 2) Finite element modelling, which has been applied to model the reconstructed stress fields; and,
- 3) The concept of stresses induced by lateral variations of density in the crust of the Earth. This concept has been incorporated in the numerical modelling of the stress field. After a short outline of the theory behind the concept, results will be presented in order to elucidate the sensitivity of the analysis with regard to the input data and applied calculations.

2.1 Stress in the Earth's crust

Planet Earth has been cooling since its formation [Sclater *et al.*, 1980]. Driven by temperature differences related to this cooling, convection cells of mantle material drag along the lithosphere plates that move relative to one another. Formation of new crustal material and divergent motions along spreading mid-ocean ridges are compensated by material returning into the deeper levels of the Earth along convergent subduction zones. Oceanic crust is dense and, therefore, can be subducted whereas more buoyant continental upper crust in general is not recycled to mantle levels. Differential motions between plates define the actual state of stress in the lithosphere. Stress leads to deformation, the type or intensity is depending on the strength of material of which the crust is composed (the combination of rheology and thickness of stronger and weaker layers, e.g. Ranalli & Murphy [1987]).

Observations of stress are limited to the outer part of the Earth and are always indirect, because only strain (deformation) is observed. Using concepts linking deformation (strain) through rheology (material parameters, depending on physical conditions) to stress, the stress field can be inferred from these observations. Principal sources of information about stress in the crust are:

1) *kinematic indicator data e.g. fault slip*

The so-called 'fault inversion method' [Angelier, 1994] uses markers on fault planes to infer the direction of their movement. It is the only method to obtain quantified information on the orientation of paleostress regimes and will be discussed in section 2.2.

2) *borehole break out data and stress relief measurements*

Both techniques are closely linked to drilling techniques. Borehole breakout data are instabilities (breakouts) in the walls of drill holes. Logging devices scan the originally circular drill holes for failures of the borehole wall and general shape of the hole. From the orientation of these observations, the orientation of the maximum horizontal compression (Sh_{max}) can be determined. For a more detailed description on this relation between maximum horizontal stress directions, borehole instabilities and tectonic regimes see e.g. Schindler *et al.* [1998], Appendix A of Gölke [1996] and references therein. Stress relief measurements determine the strain relaxation ('recovery of initial

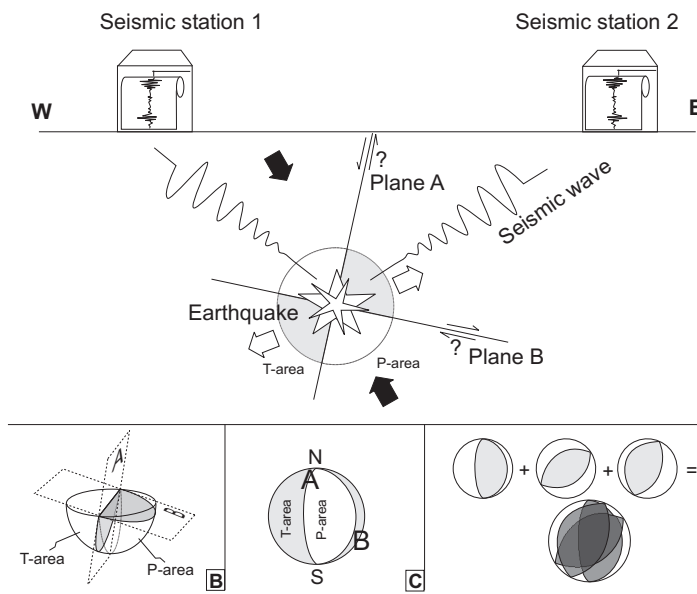


Figure 2.1.1

Schematic representation of an earthquake and the way pressure and tension axes related to the seismic event can be determined and displayed.

Panel A: Schematic E-W cross-section of an area where a hypothetical earthquake occurs due to movement along either plane A or plane B. Note difference in first arrival of the seismic waves at the seismic stations.

Panel B: 3D representation of the planes A and B from panel A and their relation to the lower hemisphere of a sphere.

Panel C: 2D representation of the lower hemisphere of panel B. This method is the stereographic method, the standard presentation for focal mechanism solutions.

form') when a rock sample is separated from the volume of the surrounding rock (if a core is taken out a drill hole). This relaxation of deformation can consequently be used to deduce the magnitude and direction of the principal axes of stress. Both these methods only resolve information about the present-day stress field.

3) earth quake focal mechanism solutions

Focal mechanism solutions use the first arrival of seismic waves produced by earthquakes (see Figure 2.1.1) to determine the orientation of the principal axes of stress. This first arrival (P-wave) has either compressional or dilatational polarity. Even without knowing which of the perpendicular planes (A or B in Figure 2.1.1) has moved, the quadrant in which the maximum compression should be located to produce movement of the fault can be calculated. The P (pressure) axis will be located in this quadrant (white in the Figure), whereas the T (tension) axis is in the other (gray in the Figure). The standard graphical presentation of these data is, just as many structural geological data, a projection of the lower hemisphere of a sphere. To clarify this method, Figure 2.1.1b shows the example in 3D and 2.1.1c using the stereographic projection. When several focal mechanisms in a region can be determined, the individual solutions can be combined to obtain a better constraint on the P and T directions (see Figure 2.1.1d). This is the so-called right dihedral method [Angelier & Mechler, 1977]. An advantage of focal mechanism solutions is the ability to obtain information on the stress field at deeper levels of the lithosphere.

With all of these methods to infer the stress in the Earth's crust, only the orientation and relative magnitude of the principal axes of stress (σ_1 , σ_2 and σ_3) can be determined. The ratios between the principal axes derived from their relative magnitudes are used to describe the stress fields in terms of tectonic regimes (see Figure 2.1.2). For all these methods, information can only be obtained at a local scale. Directions of stress in local settings may be related to local features such as zones of weakness, second order sources of stress, or other features that cause deviations. The World Stress Map compilation of stress indicator data ([Zoback, 1992] and <http://www-wsm.physik.uni-karlsruhe.de>) shows that although local states of stress might vary considerably, the regional stress field in tectonic plates displays a relatively homogenous pattern on the larger scale [Coblentz & Richardson, 1995].

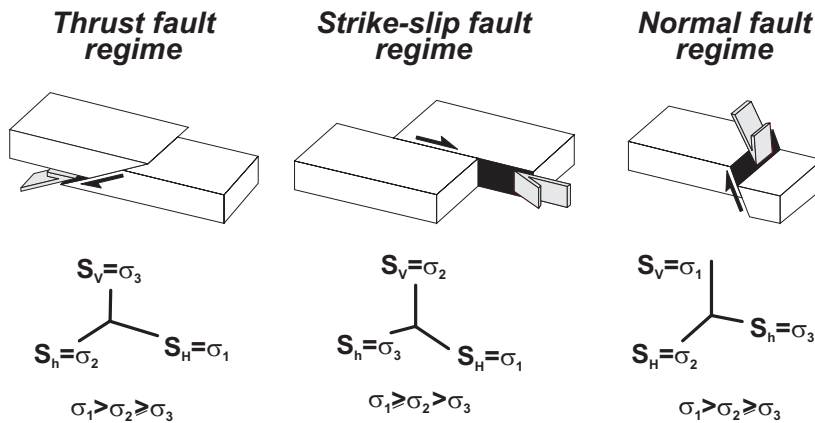


Figure 2.1.2
The three general tectonic regimes described by the orientation of the principal axes of stress. After Bada [1999].

In the World Stress Map program, solutions from fault slip inversion data are given a low quality rank. Focal mechanism solutions and borehole break out data are supposed to be more reliable [Zoback, 1992]. The fault inversion method, however, is the only way to obtain direct and quantified information about the stress field throughout geological history. Furthermore, comparison between stress trajectories obtained independently from focal mechanism solutions with the trajectories resulting from kinematic indicator data by Mercier *et al.* [1973] and SIGMA [1998] show very similar patterns. This suggests that careful analysis of paleostress regimes can provide valuable information on the orientation of the principal axes of stress for the geological past [Bergerat, 1994].

2.2 Paleostress method

Several features observed in the field can be used to infer, each in a specific way, the principal axes of (paleo)stress. These include fault-slip marks, joints and fractures (see e.g. Alsaker *et al.* [1996] and references therein), tension-structures, pitted pebbles and mechanical twinning of calcite crystals (see González-Casado & García-Cuevas [1999] and references therein). In this thesis only fault-slip marks and pitted pebbles have been used and therefore only these methods will be described in the next sections.

2.2.1 Fault inversion method

Over the last decades the fault inversion method has been applied to many regions around the world to determine the local reduced paleostress tensor for the region of interest (e.g. Angelier *et al.* [1986]; Bergerat [1987]; Bada [1999]; Simón-Gómez [1989]). A detailed outline of the method, its merits and limitations can be found in Angelier [1994]. I will only present the basic principles on the fault inversion (often referred to as 'paleostress') method.

Basics

The method is based on a rather simple concept. Consider a cube (Figure 2.2.1.1) that is subjected to a stress field. For any imaginary plane that would be cut through the cube, it is possible to determine whether and in what direction movement would occur (providing the shear stress on the plane overcomes the frictional resistance). This is the case for any orientation of compression, extension or a combination of both exerted on either side of the cube.

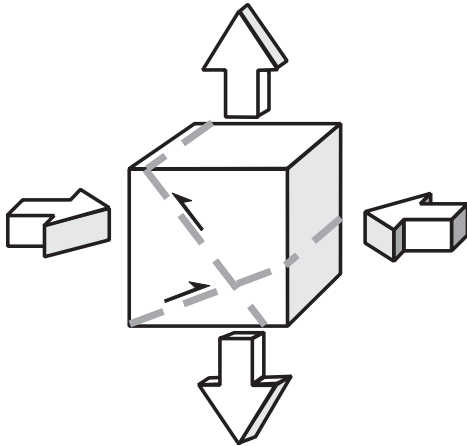


Figure 2.2.1.1

For any imaginary plane (two examples are dashed) through a cube on which stress is exerted, it is possible to determine whether and how movement would occur along this imaginary plane. The fault inversion techniques are based on the inversion of this concept. If on several, differently oriented, fault-planes movement is indicated by markers (see Figure 2.2.1.2), the orientation of the principal stresses can be determined.

Motion along fault planes often results in irregularities on the fault surface or secondary, minor faults developing due to the principal fault motion. In outcrops, different types of marks on fault planes (see Figure 2.2.1.2) allow determination of direction of motion along the observed fault plane. Both the dip and dip direction of the fault plane and the angle between the strike of the fault plane and the direction of movement in the plane can be measured. With enough data, the concept described above can be inverted (the reason why the method is called fault slip inversion) to obtain the orientation of the principal stress axes that produced the observed movement along the fault. To get a confident solution [Delvaux, 1993], information should be obtained for a certain minimum of faults with different orientations. This minimum number of observations depends on the typical setting. Mathematically, four faults would be sufficient, but depending on the type of fault-activity (reactivation, new formed faults, strike-slip or dip-slip faulting) this can vary from 6 to 15 faults. For a set of observed faults it can be determined for which combination of orientation of compression and/or extension an optimum is reached between explaining a maximum number of fault-motions and obtaining a minimum error between theoretical direction of slip (α in tables) and observation. The absolute value of these stresses cannot be computed, but the ratio between the stresses in the three perpendicular directions provides information about the type of stress field (see Figure 2.1.2) that would be able to produce the observed deformation. This ratio is expressed as R, which is defined by $R = (\sigma_2 - \sigma_3) / (\sigma_1 - \sigma_3)$.

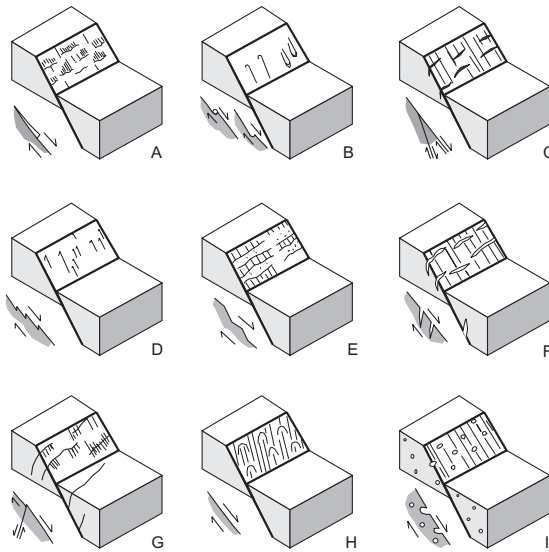


Figure 2.2.1.2

Different types of markers on fault planes that enable determination of sense of movement along the planes:

- a) accretionary mineral steps, b) tectonic tool marks, c) Riedel planes, d) stylolithes, e) stepped surfaces, f) tension gashes, g) conjugate shear fractures, h) slickensides, i) other criteria. After Angelier [1994].

the reason why the method is called fault slip inversion) to obtain the orientation of the principal stress axes that produced the observed movement along the fault. To get a confident solution [Delvaux, 1993], information should be obtained for a certain minimum of faults with different orientations. This minimum number of observations depends on the typical setting. Mathematically, four faults would be sufficient, but depending on the type of fault-activity (reactivation, new formed faults, strike-slip or dip-slip faulting) this can vary from 6 to 15 faults. For a set of observed faults it can be determined for which combination of orientation of compression and/or extension an optimum is reached between explaining a maximum number of fault-motions and obtaining a minimum error between theoretical direction of slip (α in tables) and observation. The absolute value of these stresses cannot be computed, but the ratio between the stresses in the three perpendicular directions provides information about the type of stress field (see Figure 2.1.2) that would be able to produce the observed deformation. This ratio is expressed as R, which is defined by $R = (\sigma_2 - \sigma_3) / (\sigma_1 - \sigma_3)$.

type of stress field (see Figure 2.1.2) that would be able to produce the observed deformation. This ratio is expressed as R, which is defined by $R = (\sigma_2 - \sigma_3) / (\sigma_1 - \sigma_3)$.

Temporal constraints on stress fields

From a combination of structural and stratigraphic information, upper and lower time limits can sometimes be placed upon stress fields and changes in stress fields through time can be observed. Figure 2.2.1.3 shows this in a very schematic, idealized and theoretical situation. Such ideal conditions are, however, quite rarely available. Where such conditions are not fulfilled, dating of superimposed paleostress fields becomes a major issue, see Hancock [1994].

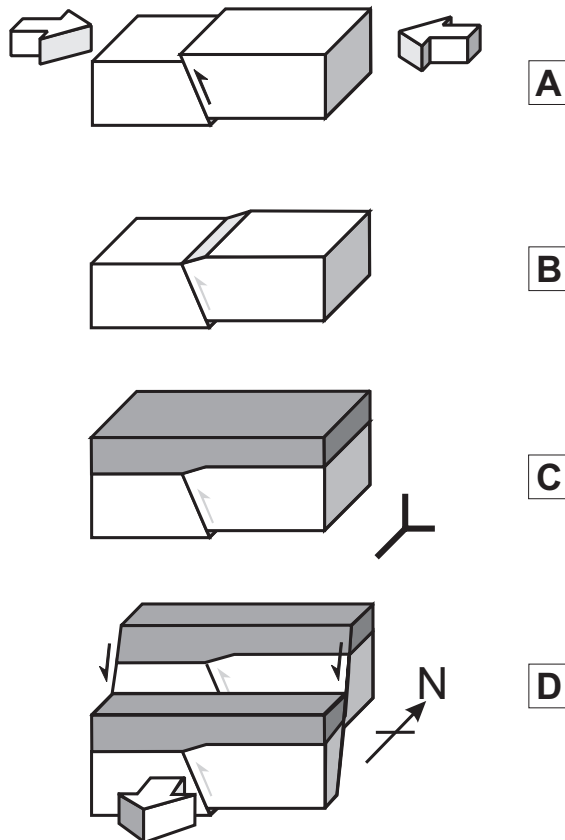


Figure 2.2.1.3

Theoretical example to explain how it is possible to determine changes in the stress field through geological time. In the example an E-W compression phase (panel A) is resulting in thrusting along a fault plane perpendicular to the maximum compression direction, throwing up the hanging wall of the fault. A period of erosion (panel B) and a subsequent stage of deposition (panel C) result in leveling of the fault scarp and sealing of the fault, respectively. After this, an extension oriented N-S leads to the development of normal faulting (panel D). In this way, the lower block will contain deformation related to both stress regimes, while the upper layer will testify that the compression took place before and the extension after its deposition. If the stratigraphic ages of both sequences are known, upper and lower time limits can be placed upon the stress fields.

Limitations

Several basic assumptions are imposing limitations on the concept:

(1) The mathematical definition that the three stress-axes are supposed to be orthogonal. In most methods, one of the principal axes of stress is supposed to be oriented vertically; the other two are in the horizontal plane (the so-called “Andersonian state of stress” [Anderson, 1951]). In reality this does not have to be the case.

(2) The cube is made of isotropic material. Applying the paleostress method, deformation is linked to stress through the material properties of the deformed medium. In practice, geological materials most often are not homogeneous at all and/or contain pre-existing weakness zones, such as bedding planes or inherited faults. Therefore, it is still a matter of debate whether the observed strain (slip along fault planes and pressure solution marks) can be related directly to regional stress regimes (e.g. Gapais *et al.* [2000]).

A further complication is the scale dependence. A minor volume of rock might be homogeneous and isotropic, but in a regional study inhomogeneities and anisotropies will occur in the rocks considered. Furthermore, large-scale structural inhomogeneities (anisotropies) affect the local directions of the stress field (e.g. Rebaï *et al.* [1992]). It is

well known that close to fault zones (whatever their size), the principal stress axes experience rotation (e.g. Casas-Sainz & Maestro-González [1996]). The same holds, although to a lesser extent, for any weak zone and rheological contrast (which shows in e.g. cleavage angle difference between shale and sandstone).

For a larger region however, rather consistent and reproducible patterns of stress orientations are observed, so deviations from the regional stress field by large-scale weakness zones can be detected [Maestro González & Casas Sainz, 1995; Zoback *et al.*, 1982].

(3) It is assumed that observed movements along the faults occurred during a single deformation event. To explain the problem involved when several deformation events have occurred, see again the example presented before (Figure 2.2.1.3). If in a subsequent stage the top of the entire sequence is being eroded, the lower layer will contain 2 stress stages, but it cannot be determined directly that these were originally two separate events. In the example, this might result in a misinterpretation of the deformation to have been formed under a single strike-slip field.

In many geological cases it is not straightforward from outcrop observation whether the rocks have been deformed by a single event or in multiple stages under possibly different orientation of the main stress field. Or more general: different reduced stress tensor of which the effects cannot be distinguished on the scale of the observation. In order to discriminate different fault sets and to minimize the subsequent error in the calculation of the stress tensor, the approach shown in the flowchart (Figure 2.2.1.4) is used.

During observation in the field, sets of faults belonging to different systems are separated as far as possible into different groups. Plotting faults and striations in stereographic projection and in rose diagrams can help to constrain the fault sets better and to assign additional faults to the subsets. Another tool to group different types of faults (normal, strike-slip, inverse) under a single direction of maximum horizontal

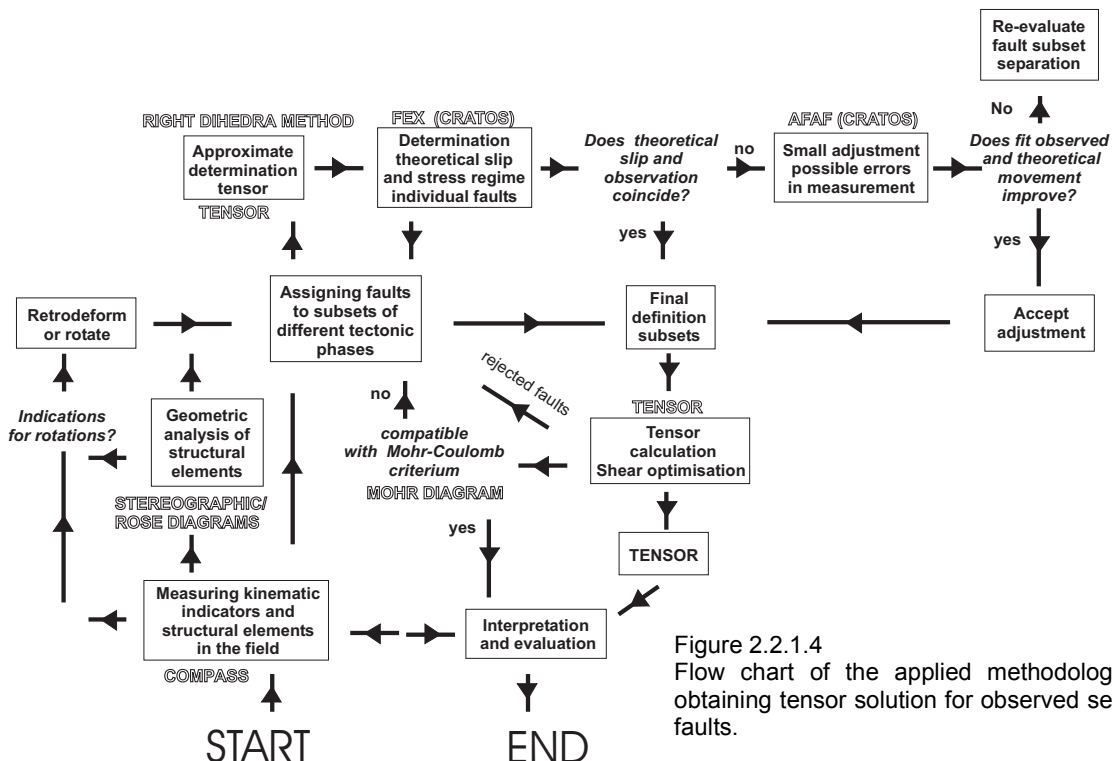


Figure 2.2.1.4
Flow chart of the applied methodology in obtaining tensor solution for observed sets of faults.

compression is the K/dy diagram by De Vicente [1988]. This method can provide theoretical movement for faults with observed orientation of movement but unknown sense.

(4) After the fault movement, the observed rock mass did not experience block rotation. In case of moderate deformation, block rotations can result in a tilt (along an axis in the horizontal plane) or spin (along a rather vertical axis) of the original orientation of the kinematic indicator data. The latter can be constrained by paleomagnetic data. Whenever indications from the field suggest late stage tilting of the observed outcrop, the observed kinematic indicator data should be rotated back to the orientation under which they have been formed originally. In some cases a post-fracturing rotation along a horizontal axis can be derived from the resulting stress field, if a consistent solution is obtained for which the principal stress axes are tilted with respect to the horizontal.

(5) The rock mass moved rigidly along the discrete fault planes. Numerical experiments by Dupin *et al.* [1993] show that if numerous data are used and fault spacing is large, the assumption of rigid discontinuous rock mass behavior does not affect the resulting stress calculations to a great extent.

Numerical experiments have been applied to prove that some of the previously mentioned assumptions of the fault inversion method are not valid in some cases. Cashman & Ellis [1994] showed that multiple striations on a single fault surface can result from the interaction of faults during a single deformation event in a zone with a complex fault pattern and need not reflect major changes in the stress field, as they are often interpreted. Another experiment examining the discrepancy between directions of maximum shear stress and predicted slip on fault planes in fault systems with different orientations came to similar conclusions [Pollard *et al.*, 1993]. These numerical studies show that the relation between fault slip data and stress orientations should be considered with some caution. Application of the results of the numerical studies would require a very detailed knowledge of weakness zones present in the area of study. To determine this for a present-day setting is difficult, let alone for the geological past.

2.2.2 Striations and solution pits on pebbles

Pitted surfaces on pebbles in conglomerates have long been observed and have been attributed to pressure solution (e.g. Trurnit [1968]). Sanz de Galdeano & Estévez [1981] demonstrated that, together with scratches on the pebble surface (resulting from relative movement along the matrix-clast contact), these pressure solution features can be used as kinematic indicator data to determine the orientation of regional compression. See Figure 2.2.2.1 for an example of a pebble with kinematic indicators. The process of forming kinematic indicators on pebble surfaces in a matrix is favored by (amongst others) (a) the presence of interstitial water, (b) an important difference in size between pebble and matrix grains and (c) a high contrast in hardness between matrix and pebbles components. E.g., limestone pebbles in a matrix containing quartz grains are very likely to develop striations and pressure solution features. When compared with 'traditional' fault slip inversion, the orientation of the maximum compression obtained by the kinematic indicators on pebbles provides very similar results ([Estévez & Sanz de Galdeano, 1983] for the Granada and Guadix-Baza basins). To produce these features relatively limited compression is required [Sanz de Galdeano & Estévez, 1981]. This makes the kinematic indicators on pebbles ideal to determine the orientation of regional compression in neotectonic studies for areas where other kinematic indicator data are less well developed or absent.

Several methods have been proposed to determine the orientation of the principal stress axes from the deformation of pebbles in a conglomerate:

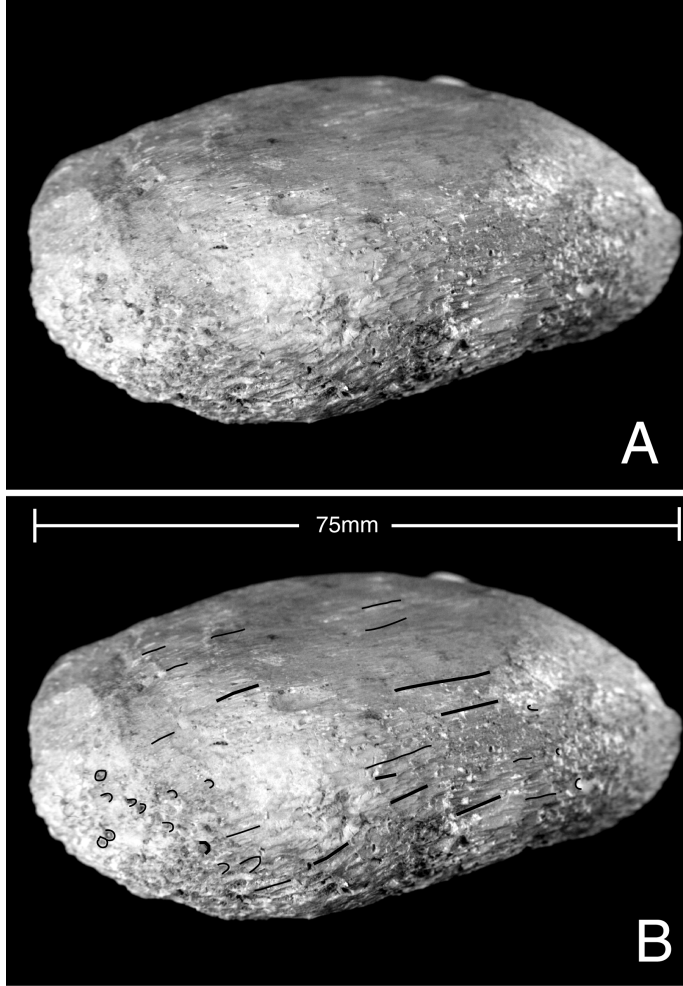


Figure 2.2.2.1
Panel A: carbonate pebble from outcrop near Ponferrada (NW Iberia) showing pressure holes and scratches by quartz grains, indicating direction of direction of maximum compression (σ_1). Panel B shows interpretation.

(1) Sanz de Galdeano & Estévez [1981] used the conical distribution of the striations, converging to 2 opposite poles where dissolution is maximal. The orientation of the line connecting both poles is measured and is supposed to coincide with the maximum compression direction. Estimates for the other principal axes are not provided by this method.

(2) Schrader [1988] describes a measurement technique putting the pebble into a system of spatial polar co-ordinates in its in situ orientation. The features on the pebble are measured in spherical angles with respect to the origin: the shape of the pebble is neglected. For near spherical pebbles deviations are small. The maximum direction of compression is measured directly on the pebble; the orientations of the intermediate and minimum compression axes are derived from the trace of the striations on the surface of the pebble.

(3) Taboada [1993] proposes that the striations and polished surfaces on a single pebble can be treated as a set of faults developed by the local stress tensor around the spherical body or the displacement tensor

between the pebble and the matrix. This means that measuring the orientation of the observed striations on the pebble surface would provide an 'ideal' set of measurements for the fault slip inversion method. This allows for the determination of the orientation of all three principal stress axes. The method is a theoretical and graphical method to obtain the trajectories of the striations on the surface of a pebble, projected on a sphere.

Rodríguez Pascua & De Vicente [1998] found very similar results for the methods of Schrader [1988] and Taboada [1993] for an extended data set of pitted and scratched pebbles from the Zaorejas basin. Since the method by Schrader [1988] is more practical in use, this method is preferable, as long as pebbles are as spherical as possible.

2.2.3 Regional context and (paleo)stress trajectories in Iberia

Results of paleostress studies should be correlated carefully with regional data on meso- to macro scale structural elements in order to evaluate the regional meaning of the obtained results and in order to date its timing. An example of how important it is to interpret local results in a regional context is the Madrid Basin (MB).

The intraplate Cenozoic Madrid Basin forms part of the Tajo Basin, located in the central part of Spain (see Figure 2.2.3.1). Its northern border is formed by the Spanish Central System (SCS), an intraplate mountain range with present elevation up to 2600m, standing up to 2000m above the basin. The development of this intraplate mountain range is due to multiple reactivations of late Hercynian basement faults. Most important has been the flexural response to southward thrusting of the Spanish Central System. In chronological order the development of the basin can be described as follows. During the Paleogene WSW-ENE trending boundary faults of the SCS favored sinistral strike-slip movement under the NNE-SSW compression of the Pyrenees [Vegas *et al.*, 1990]. In the north-eastern part of the SCS this led to a transpressive setting causing flower-type structures, which can be documented in the thin Mesozoic cover and early Paleogene sediments (see Chapter 3). Under this compressional stress regime, the Iberian Chain (IC) thrust onto the NE basement of the MB. Deformation continued later under an approximately E-W compression which resulted from the superposition in place and time of the Pyrenean and Betic compression, forming the Sierra de Altomira [Muñoz Martín *et al.*, 1998]. Upon waning of the Pyrenean compression, the situation reversed: the IC became a major dextral strike-slip zone (lateral offset estimated up to 35km, [Bergamín *et al.*, 1996]) whereas the border faults of the SCS were oriented in favor of thrust-faulting under the Betic NNW-SSE compressional stress field. The flower-type inheritance of the SCS (see Chapter 3) favored the popping up of the mountain belt during M. Miocene. The Southern Boundary Fault (SBF) was dipping steeply, thus creating an active type of basin setting. The uplift, loading by southward thrusting of the SCS, and sedimentation created a deep foreland basin containing 2000-3500m of sediments of predominantly Late Paleogene-Late Miocene age [Querol, 1983]. The active southward thrusting of the SCS seems to have ended at around Pliocene, ongoing tectonic activity seems to be restricted to second order strike-slip faults that cut the ancient thrust front.

Paleostress studies by De Vicente *et al.* [1996b] show an abundance of deformational structures in M. Miocene to Quaternary sediments in the central part of the MB on different scales. Both numerous paleostress tensors deduced from fault-analyses in M. Miocene-Quaternary sediments within the MB and focal mechanism solutions indicate the presence of two contemporaneous stress fields active from M. Miocene to present: NNW-SSE compression and sub-parallel NNW-SSE extension [De Vicente *et al.*, 1996b].

Presently the major thrust front of the SBF is bisected by smaller strike-slip faults trending NNE (sinistral) or NW (dextral). Part of the seismic activity along the southeastern border of the SCS seems restricted to these strike-slip faults (see Figure 2.2.3.1). Distribution of seismicity in the MB is restricted to a very well defined zone, trending approximately parallel to the SCS, some 50-70 km to the south of the major thrust front, coinciding with the location of the flexural bulge of the SCS-MB Miocene foreland system. In this region, the major valleys show obvious straight traces, bounded by normal faults (see Figure 2.2.3.1) creating hanging valleys on either side.

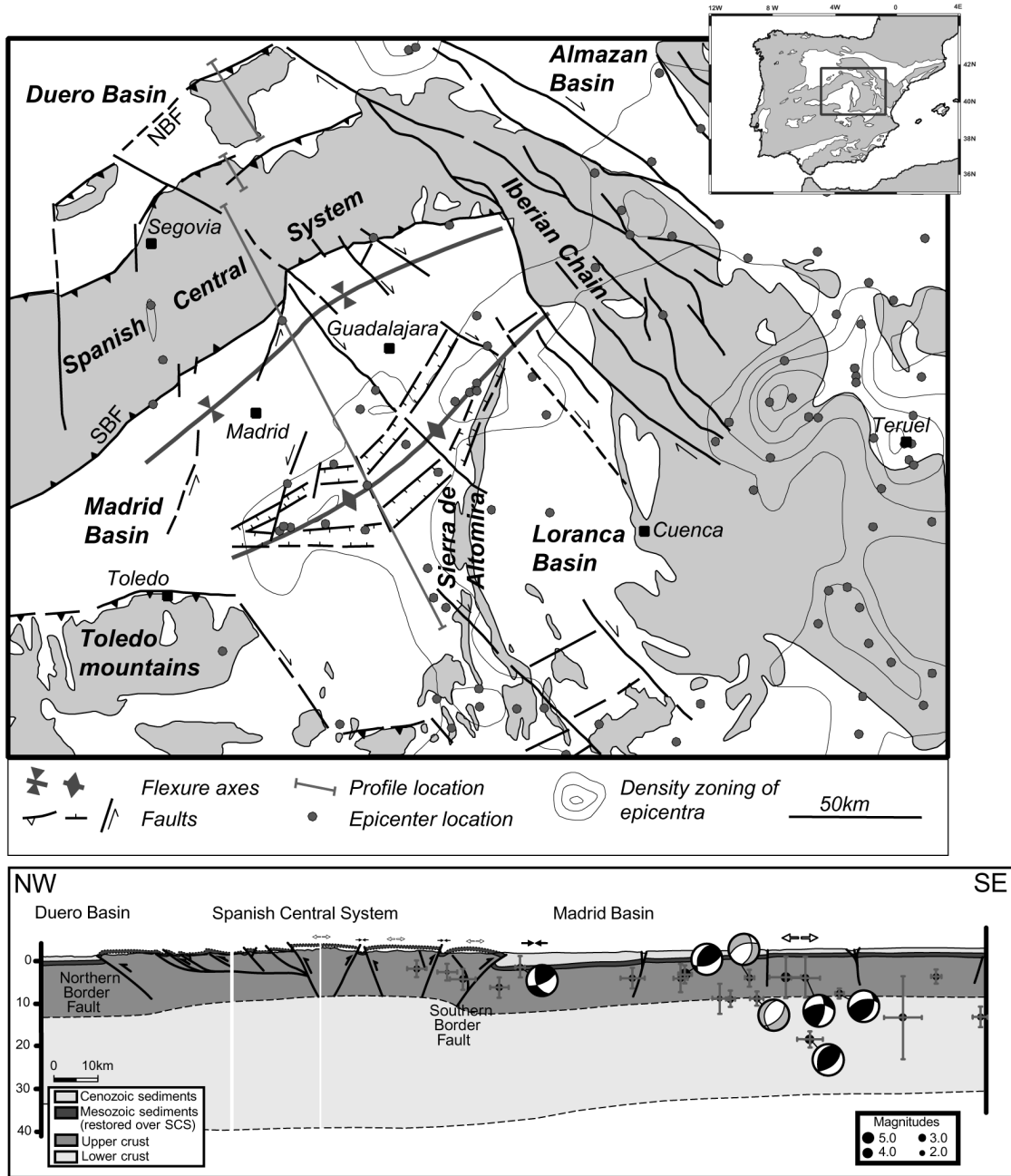


Figure 2.2.3.1

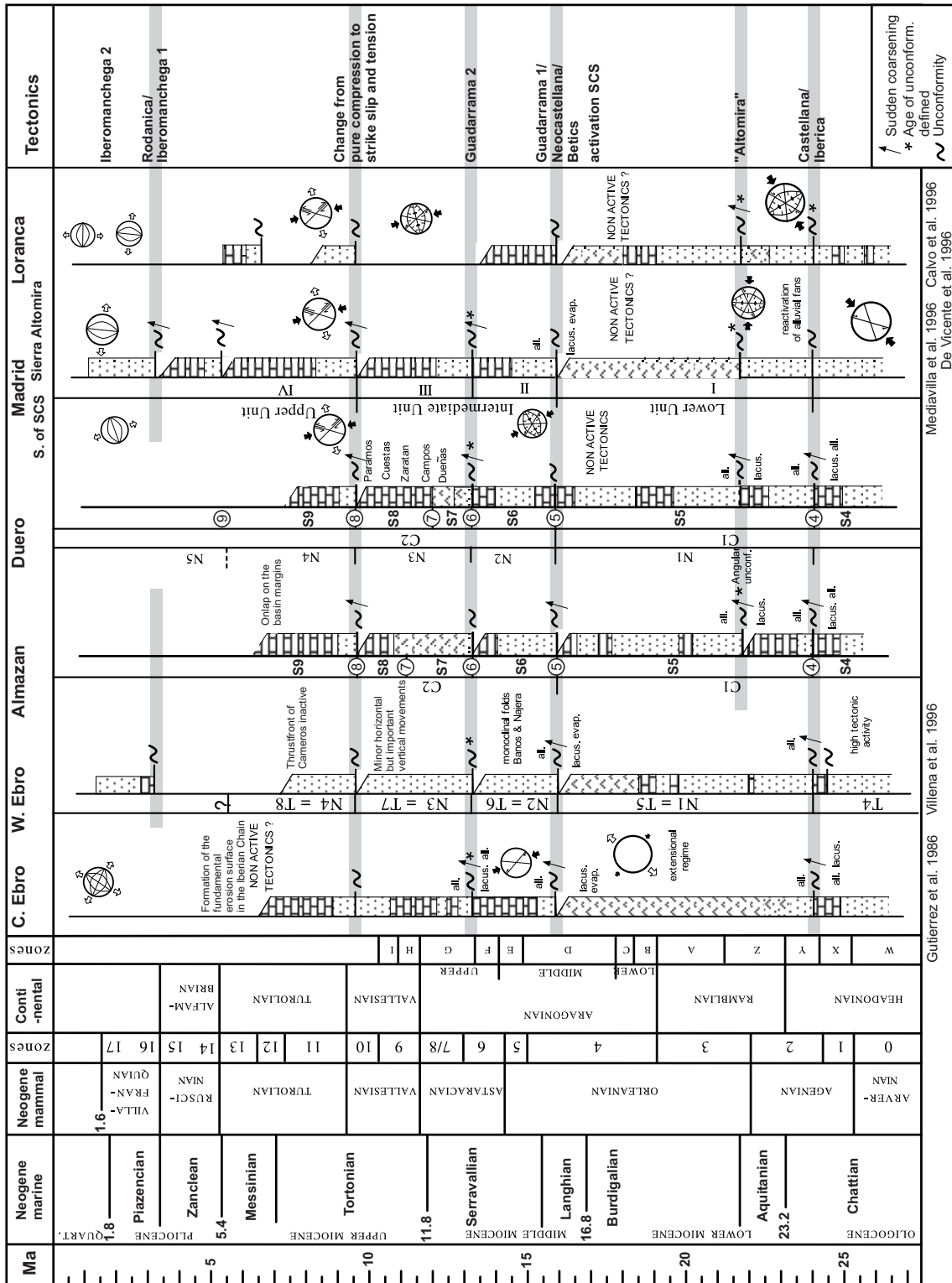
The neotectonic setting of Central Iberia shows a set of intraplate mountain ranges (Spanish Central System, Iberian Chain) separating extensive basins (Duero Basin, Madrid Basin).

Upper panel: rejuvenation of the flexural bulge related to the M.Miocene southward thrusting of the SCS [Van Wees et al., 1996] is suggested by the distribution of seismicity (red dots) and normal faulting. Present-day activity of the Southern Border Fault of the SCS is restricted to strike-slip faults bisecting the major thrust front.

Lower panel: cross section through the SCS and MB along profile line in upper panel, showing projected earthquake locations (with error bars) and available focal mechanism solutions. The arrows indicate superficial local stress fields.

Deformation of Quaternary sediments is restricted to the same zone as the seismically active area. Large parts of the focal mechanism-solutions are compatible with an overall NNW-SSE compression related to ongoing convergence between Africa and Iberia, whereas some indicate extension exactly parallel to this overall compressional direction [De Vicente *et al.*, 1996b]. These findings are compatible with flexural upbending of the lithosphere causing extensional bending stresses at shallow levels, whereas at depth compression will prevail below a neutral surface. Although more data on focal mechanisms are required to support this hypothesis, projection of the known focal mechanisms onto a cross-section seems to indicate a vertical separation between the extensional and compressional earthquakes (see lower panel in Figure 2.2.3.1). The neutral surface in this case, is due to scarceness of data, lateral projection and errors in focal depth determination not well defined. However, the lower panel of Figure 2.2.3.1 shows that the shallowness of several compressional events point to a neutral surface around 5-7km. This seems to be in the same order as the EET (Effective Elastic Thickness) value of 7km obtained by flexural basin modelling [Van Wees *et al.*, 1996]. This value, however, might be an underestimate, since the spatial distribution of present-day seismicity and Quaternary deformation indicates a present amplification of the initial foreland-bulge of the MB-SCS due to intraplate compression. Therefore, the present-day curvature of the plate should not be considered as the result of flexural loading by the SCS only. The extension parallel to the regional compression in the MB can be explained as a superficial expression of the overall NNW-SSE compressional regime active in central Iberia from about Middle Miocene to present-day and should therefore not be regarded as the expression of a distinct extensional phase. Rather it should be attributed to the effect of flexural bending stresses resulting from regional compression. As described before, differential movement between Eurasia, Africa and Iberia, due to the progressive opening of the Atlantic, is reflected in Iberia by changing Tertiary stress fields. Numerous Tertiary intracontinental basins have been formed and subsequently deformed as large Late Hercynian basement faults were reactivated multiple times under these stress field changes. In this way, the infill of these basins and uplift of their borders have (indirectly) recorded changes in plate boundary activity of the Iberian plate and provide indirect information on these changes. Figure 2.2.3.2 shows a rough correlation of major unconformities and tectonic events for the larger basins in northern and central Iberia.

The Tertiary basins in Iberia form good sites for paleostress studies, as their infill is episodic and young. The latter implies that the sediments witnessed only the last few deformational stages, which makes it easier to distinguish them. Moreover, in many of these basins, Tertiary sediments are deformed. Along the borders of the basins this deformation can be very pronounced. Away from the active borders, deformation becomes moderate, forming abundant deformational structures without large-scale rotations, satisfying some of the basic assumptions of the paleostress method. The internal structure of the sedimentary infill, imaged by reflection seismics (e.g. Querol [1983]; Pulgar *et al.* [1997]; Sabat *et al.* [1995]), contains a large body of information on the tectonic history of the basins and the areas bordering them. On basin wide scale, local stress fields are documented very well, both in time and place. For Central Spain (e.g. De Vicente *et al.* [1996b]; Muñoz Martín [1997]), the Betic region (e.g. De Ruig [1990]; Stapel *et al.* [1996b]; Huibregtse *et al.* [1998]; Jonk and Biermann [2001]), the Iberian Chain (e.g. Simón-Gómez [1989]), Ebro Basin and southeastern foreland of the Pyrenees (e.g. Guimerà [1984]), a considerable amount of data has been gathered and published.



Gutierrez et al. 1986 Villena et al. 1996
 Mediavilla et al. 1996 Calvo et al. 1996
 De Vicente et al. 1996

Figure 2.2.3.2

Tentative correlation between stratigraphy in the large Cenozoic basins of Central Iberia, tectonic events (rightmost column) and stress fields. Several events can be recognized in major part of the basins (e.g. the breaks in sedimentation in the Middle and Late Miocene), but regional events can be observed as well (e.g. the absence of the Aquitanian "Altomira" event in the Ebro Basin). Based on a Figure by Calvo et al. [1993]. Stress field results added from Gutierrez et al. [1986]; Villena et al. [1996]; Mediavilla et al. [1996]; De Vicente et al. [1996]. Abbreviations in Figure: all. = alluvial, lacus. = lacustrine, evap. = evaporitic.

A major problem in reconstructing stress fields in Iberia at larger scale through time is the age of observed deformations. Dating of a specific sedimentary interval containing the kinematic indicator data is in many of the Tertiary basins very difficult because of the lack of good biostratigraphic markers in their predominantly continental sedimentary fill. Rodent teeth dating (see Daams *et al.* [1996] and references therein) combined with magnetostratigraphy [Krijgsman *et al.*, 1994] have provided the only direct dating method in continental deposits in limited areas (the Loranca Basin, the Teruel-Catalayud Basin and the Vallès-Penedès Basin [Garcés *et al.*, 1996]) and only for the Middle to Late Miocene record [Krijgsman *et al.*, 1996]. These studies should be expanded to other time intervals and basins in the Iberian Peninsula.

In the larger Duero, Tajo and Ebro basins, the continental sediments along the basin margins grade towards the basin center into lacustrine sediments that can be dated. Lateral correlation to the continental sediments provides a widely applied method of indirect dating. In the numerous smaller, isolated intramontaine basins (e.g. Bierzo, Guadiana, Zaorejas, Avila and Lozoya) where datable lacustrine sediments are scarce or absent, the absolute dating of the Tertiary (?) sediments is poor. As a best approximation these sediments are correlated based on their nature (fluvial; distal or proximal) and lithology (red conglomerates, silts, sands and clays) with better age-constrained series of larger basins (e.g. Martín Serrano *et al.* [1996]). Fortunately, the littoral basins (e.g. Emporda, Maestrazo, Vallès-Penedès, Lusitania) and the basins within the Subbetic and Betic Cordillera (e.g. Vera, Sorbas, Nijar) are characterized by several marine ingressions and, therefore, dating is much more precise in these regions.

Yet, even if sediments and stress field changes can be accurately dated (e.g. Huibregtse *et al.* [1998]; Stapel *et al.* [1996b]), correlation of deduced stress tensors over larger distances is not very straightforward. A compilation of the paleostress data along a NE-SE oriented 'profile' (see Figure 2.2.3.3) in the Iberian Peninsula shows that the stress field was far from homogeneous and underwent several considerable changes during Tertiary to recent times. This is yet another reason why correlation of 'tectonic phases' between regions based on local stress-fields is difficult. Several authors have, however, succeeded in reconstructing regional (paleo)stress fields for Iberia and surrounding areas over limited time intervals. Examples are (1) Eocene-Oligocene of the Ebro basin and Catalan Coastal Ranges (e.g. Guimerà [1984]), (2) Late Miocene to present-day in the Iberian Chain [Simón-Gómez, 1989], (3) Middle Miocene to present-day in the Madrid and Loranca basins [De Vicente *et al.*, 1996b], (4) Middle Miocene to present-day for the Betic-Rif Cordilleras [Galindo-Zaldívar *et al.*, 1993], (5) present-day on- and offshore Portugal [Ribeiro *et al.*, 1996], (6) Eocene to Miocene of the Alpine foreland [Bergerat, 1987], (7) present-day Iberia [Andeweg *et al.*, 1999a], based on limited information (focal mechanism solutions, borehole breakout data and Quaternary fault slip data) by e.g. De Vicente *et al.* [1996b] and (8) present-day Iberia [SIGMA, 1998]. Updated with, amongst others, information that will be presented in Chapter 3 of this thesis, a more up to date compilation of the available data for the recent and present-day stress field in the Spanish part of the Iberian Peninsula has been completed. Encompassing an enormous number of over 105.000 fault slip and 156 focal mechanism solution data (including results of work presented in this thesis), within this Spanish national compilation two independent maps have been constructed using either of both sources of information. The resulting trajectories of S_{max} do not differ much from the early version by Andeweg *et al.* [1999a]. By constructing two independent maps based on either source of information (Focal mechanism and fault slip data), the resulting differences of stress trajectories could be compared. At the scale of the entire Iberian Peninsula differences between the stress patterns turned out to be of minor

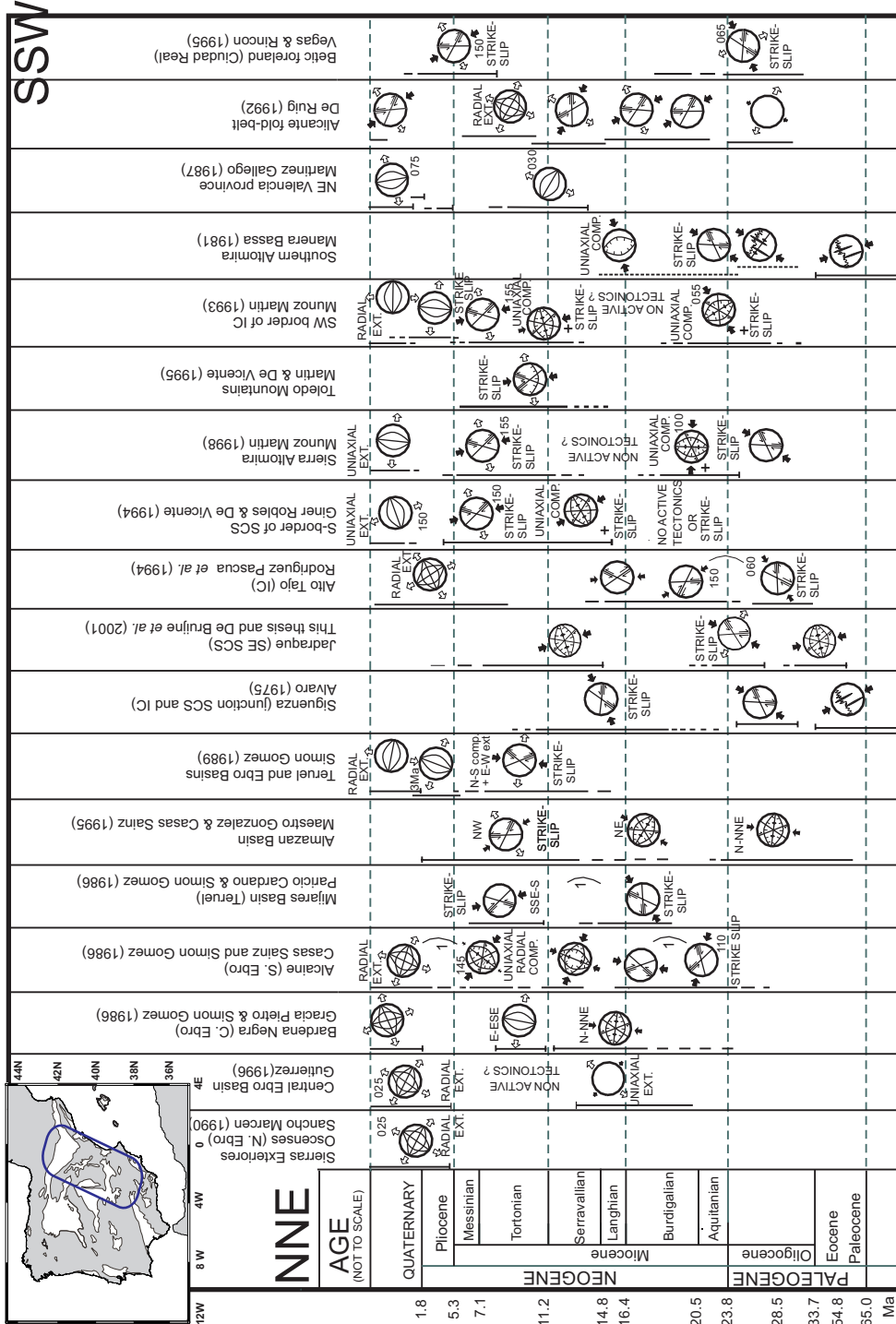


Figure 2.2.3.3 Tentative correlation between several paleostress studies in the Eastern Iberian Peninsula, arranged in a profile-like way from north (Southern Pyrenees) to south (Betic foreland). Note that correlation between stress fields is restricted to regions. In other words: different states of stress coexist in time for different regions in the Iberian Peninsula. This illustrates the need to put the paleostress data in regional and temporal context to understand the development of the regional stress fields. Data from Sancho Marcen [1990]; Gracia Prieto & Simon Gomez [1986]; Casas Sainz & Simón Gómez [1986]; Paricio Cardano & Simón Gómez [1986]; Martín Velázquez & De Vicente [1995]; Manera Bassa [1981]; Vegas & Rincon [1996]; Giner Robles et al. [1994]; Rodriguez Pascua et al. [1994]; Muñoz Martin [1993]; Muñoz Martin [1997]; De Ruig [1991]; Alvaro [1975]; Gutierrez [1986]; and Andeweg [this thesis, Chapter 3].
 1) = permutation of principal axes of stress likely.

importance [SIGMA, 1998]. The minor differences between both results for the recent and present-day stress field, suggest once more that the use of fault slip data for the reconstruction of paleostress fields in the geological history can provide stress trajectory maps with reasonable results at larger scale. In this way, the results from a large database of fault slip data can provide indirect constraints on plate boundary processes that were active through geological history.

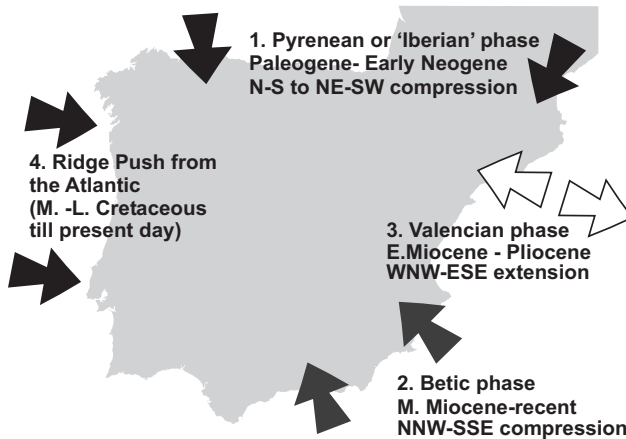


Figure 2.2.3.4

Although temporal and spatial differences occur between local and regional states of stress, the development of the stress field in the Iberian Peninsula is related to four major sources of stress, overlapping in time and place (see text). The resulting changes in the intraplate stress have caused polyphase fault reactivation under different stress fields, basin formation and deformation, vertical motions, erosion and sedimentation.

In general, however, it is clear that throughout the Tertiary the paleostress field in the Iberian Peninsula must be related to the following active first order far field stress sources (see Figure 2.2.3.4): (1) Collision of Eurasia and Iberia, resulting in the development of the Pyrenees along the north of the Iberian mainland (Paleogene - E. Miocene), (2) Collision between Eurasia (Iberia being incorporated) and Africa through the Alboran microplate, creating the Betic Cordillera in the southern part of Iberia (M. Miocene - present-day), (3) Extension to the east of Iberia resulting in opening of the Valencia Trough (Oligocene - M. Miocene, resuming in Pliocene times), (4) Progressive opening of the Atlantic to the west of the Peninsula (Late Mesozoic - present-day).

From these different sources stresses were transmitted to the interior of the relatively small Iberian Peninsula. Some of the plate boundary processes were active only during a (relatively) short time span and changed in sign, magnitude and direction rapidly. This resulted in temporal and spatial superposition of the stresses leading to local stress fields with Sh_{max} orientations changing within several hundreds of kilometers.

The Sierra de Altomira presents a nice example of this principle of superposition of far field stresses. This N-S trending fold-and-thrust belt in Central Spain (see Figure 2.2.3.1) is a somewhat enigmatic feature: while the overall tectonic setting in the Iberian Peninsula was N-S oriented compression, the Sierra Altomira extruded towards the west from Late Oligocene - Early Miocene [Muñoz Martín, 1997]. The active period of this structure is well constrained to the latest Oligocene-earliest Miocene: Upper Oligocene sediments deformed in the structure, Lower Miocene sediments that onlap the Altomira structures seal the structure [Gomez *et al.*, 1996]. During the onset of deformation the Pyrenean collision was still active, resulting in NNE-directed compression in at least NE Iberia [Guimerà, 1996]. For the latest stage of deformation (Middle Miocene) the approximately NNW Betic compression is inferred to have been the dominant stress field [De Vicente *et al.*, 1996b]. The extrusion to the west of the Sierra de Altomira occurred under N100 directed compression, documented as the "Altomira" stress field [Muñoz Martín *et al.*, 1998]. The local geological setting facilitated this extrusion, faulting and folding. A basement fault was active as a normal fault during the Mesozoic, resulting in a

western culmination of a decollement level, the plastic facies of the Upper Triassic (Keuper) [Querol, 1983]. In the subsequent compressional stage both features (the basement step and culmination of the decoupling layer) generated stress concentration at the tip of the basement fault ([Van Wees *et al.*, 1996]; [Muñoz Martín, 1997]) and decoupling was restricted to the downthrown block only (where Keuper facies was present). Finite-element studies have reproduced the N100E compression required for the observed deformation in the Sierra de Altomira region by applying a remnant of the Pyrenean compression from the north and the onset of Betic compression from the south [Muñoz Martín *et al.*, 1998]. This explanation of the development of the Altomira structure points to a gradual change in the active plate boundaries through time, during which superposition of the Pyrenean, Atlantic and Betic stress fields induced a locally anomalous ("Altomira") stress field in central Iberia. The thickened crust in the Pyrenean region might have played an important role in this deformation as well. Just as in the present day the influence of the Pyrenees on the local stress field of the NE peninsula can still be observed.

2.2.4 Conclusion

In spite of their low 'confidence' ranking by the WSM-classification [Zoback, 1992], and the shortcomings mentioned of the fault slip method, many regional field studies have shown fairly consistent patterns of stress orientations (for Iberia e.g. De Vicente *et al.* [1996b]; Guimerà [1996]; Simón-Gómez [1989]). For the geological past, the fault slip inversion is the most adequate way to obtain information about the paleostress patterns, provided there is an adequate sedimentary record preserved. If abundant observations and results (to eliminate statistical errors in the measuring procedure) from a large region (to eliminate local effects) are being evaluated with care and compared with well-documented active larger scale structures, the method provides valuable information [Bergerat, 1994]. A compilation of stress tensor results from kinematic indicators can be used to determine the temporal and spatial evolution of the stress field of a larger area and these changes of local stress fields and patterns of intraplate deformation provide information on plate boundary processes.

2.3 Finite element modelling of intraplate stress

Over the last decades numerical modelling of many kinds of tectonic processes has been applied on a wide range of geological problems (see for a review Cloetingh *et al.* [1998]). This range covers amongst others stress (e.g. Bada [1999]; Gölke [1996]), strain (e.g. Janssen [1996]; Spadini [1996]), extension (e.g. Van der Beek [1995]; Ter Voorde [1996]) compression, basin evolution (e.g. Lankreijer [1998]; Van Wees [1994]), sedimentation (e.g. Den Bezemer [1998]) and P-T-t modelling (e.g. Van Wees *et al.* [1992]; Willingshofer [2000]). Depending on the purpose of the study, different numerical concepts and techniques have been applied. The most adequate method to calculate stress and strain in a given material is the finite element method (FEM).

FEM is a matrix algebraic method able to compute the behavior of complex geometries composed of multiple materials that are subjected to varying boundary conditions. The method was developed early last century primarily to calculate stress and strain in civil engineering constructions, but did not become widely used since it involves inversion of matrices, which is time consuming even for small matrices. With the advance of computer power, matrix equations could be solved on small time scales, leading to an enormous development of applications for FEM. The mathematical description and the fundamental equations that constitute the matrix inversions have been described

concisely by amongst others Zienkiewicz & Taylor [1988a] and Zienkiewicz & Taylor [1988b]. Beekman [1994] discussed how the method could be used for geological deformation processes (bending, faulting and friction). Interested readers are referred to these studies and references therein for theoretical background.

The first finite element models to calculate patterns of stress in the Earth's crust were those by Richardson *et al.* [1979] in the late seventies. The models applied elastic deformation, encompassed the entire Earth and did not allow for much detail. To a first order, the modelled patterns of stress could be related to the major driving forces of the plates, in the modelling applied as boundary conditions at the edges of the plates. Vilotte *et al.* [1982] have been using a viscoplastic medium to apply the same concept to plate wide scales (e.g. the Indian-Asian collision). Wortel [1980], Cloetingh *et al.* [1982], and Cloetingh & Wortel [1986] were among the first to include more physical aspects of the forces applied to the model by considering the ridge push forces as an integrated pressure gradient due to the cooling of the lithosphere (see appendix A). These boundary forces were applied to a model with a uniform plate composed of homogeneous elastic material for the Cocos-Nazca plate and the Indo-Australian-plate. Since then, models have become more complicated, in terms of including increasingly more free parameters and concepts, like variations in material properties [Grünthal & Stromeyer, 1992], inclusion of weakness zones [Mantovani *et al.*, 2000], and different representations of applied boundary conditions and rheology. Hu *et al.* [1996] for example included elasto-plastic deformation in a geometrical complex model of Taiwan. Potential energy differences induced by lateral density variations have been incorporated in the modelling by amongst others Coblenz *et al.* [1994]. In this way, buoyancy forces related to lateral density variations and crustal topography were introduced in the modelling, using the age-depth relationship of cooling oceanic lithosphere [Parsons & Sclater, 1977]. Finally the step was made from 2D to 3D models: Gölke *et al.* [1996] presented a three dimensional model for the Norwegian margin and Ragg *et al.* [1999] did so for Sicily including domains with different material parameters.

Whereas these previous models were able to reproduce the directions of maximum horizontal compression on a large scale, the resulting local state of stress in many cases was not consistent or just not compared with observations. In the present research, the purpose is to simulate the stress fields that led to the significant intraplate deformation in the Iberian Peninsula since the Tertiary and to link deformation with vertical motions detected by fission track analysis ([De Bruijne & Andriessen, 2000; De Bruijne, 2001]). To be able to assess proximity to failure along faults with a given orientation, a better fit between the observed and modelled states of stress is required.

It should be noted that the purpose of the modelling presented in this thesis is not to mimic the real world, but to study physical processes behind the observations in the geological past. Numerous parameters that have been incorporated in previous studies (e.g. crustal composition, crustal thickness, basal drag, detailed crustal configuration etc.) cannot be constrained for the present-day, let alone for the geological past. Therefore, a model is applied with only a limited amount of free parameters, which facilitates direct understanding of the effect that different plate boundary conditions have on the resulting stress field. Furthermore, the larger the set of free parameters included in a model, the harder it becomes to draw conclusions from the model results, due to the problem of non-unique solutions. This being said, numerical modelling can provide valuable insight in geological processes and enables quantitative testing of hypotheses posed on these problems.

To be able to compare the results for the present-day stress with the paleostress field, the models in this thesis are kept as internally consistent as possible. A few parameters that have been incorporated in previous studies can hardly be constrained for the present-day, let alone for Tertiary times. Amongst these are:

(1) Basal drag along the base of the plate as it moves in an absolute reference frame over the mantle. This basal drag generally is calculated by summing the forces acting on a plate, which leads to the torque of this sum acting on the plate [Richardson, 1992]; [Meijer, 1995]. The sum of the torque and the basal drag shear forces should be equal to the absolute plate motion. For the present-day situation absolute plate motion is inferred from global models such as the NUVEL-1 model [DeMets *et al.*, 1990]. Absolute plate motion for Western Europe is extremely small (5mm/year), so it is hard to distinguish between the contributions of collisional forces and ridge push forces [Richardson, 1992]. It is, however, arguable whether basal drag calculated for the entire Eurasian plate is representative for the Iberian part of it. During the period that Iberia acted as an independent plate, basal drag might even be disregarded anyhow because small plates can be considered to be mechanically decoupled from the mantle [Melosh, 1977]. Moreover, for the reconstructions of the Iberian plate, absolute motions through time [Gordon & Jurdy, 1986] are not well documented and the estimates depend on the reconstruction model used and the relative motion vectors derived from the different rotation poles. Even for the present-day situation, differences between models observing the direction and amount of absolute plate velocity result in different values for the basal drag, see e.g. Meijer [1995]. In future studies, when more data is available on absolute motions through time, inclusion of the basal drag would help to constrain the magnitudes of the different plate boundary processes even further.

(2) The contribution of circulation of mantle lithosphere [Wuming *et al.*, 1992]. First order estimates from studies of large scale lithospheric stress induced by global mantle circulation [Steinberger, 1999] show that non-hydrostatic lithospheric stress might vary between -140 and 140 MPa. For the Iberian Peninsula values range between the low values of +40 and 0 MPa [Steinberger, 1999]. As in the case for basal drag, information of lithospheric thickness variations through time is very limited and it would be very speculative to incorporate this. Therefore it has not been included in the modelling.

(3) Zones of weakness, such as faults.

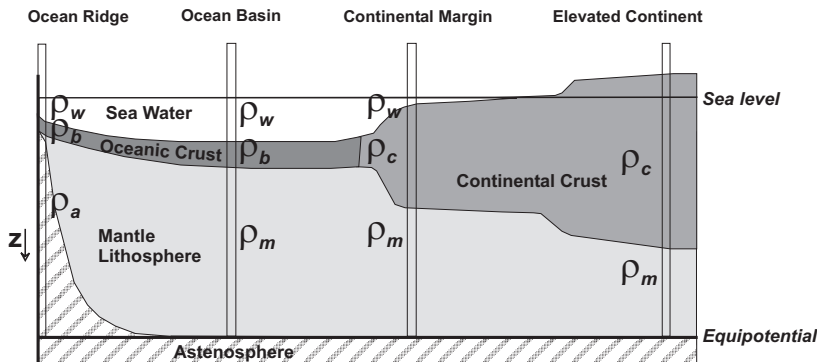
A fundamental problem is to what extent faults should be incorporated in the modelling. Should these be only the seismogenetic ones, which show seismic activity under the present stress field? Or all observed and inferred basement faults, which will constitute weakness zones as well but might not be activated under the present-day stress field? The definition of seismotectonically active faults is not straightforward, although attempts are made to generate databases on them (e.g. FAUST project, <http://faust.ismes.it/>). Even if it is possible to incorporate major faults, should not all of the small active faults be incorporated as well? The bulk deformation from very limited displacements along smaller faults is reported to be just as important as the strain accommodated by the larger structures (e.g. Sheridan [1998]). An additional major problem arises when considering the setting for geological times: how to proceed when going back in geological time and willing to determine the amount of activity of inferred faults? Until better methodologies are developed to overcome these problems, not incorporating faults seems to be the best solution for the large-scale modelling presented in this thesis.

2.4 Stresses induced by lateral density variations

Forces acting on tectonic plates can be subdivided into forces that act on the plate boundaries (e.g. collision forces) and forces acting within plates (e.g. buoyancy forces).

Gravitational body forces (i.e. buoyancy forces) play a major role in intraplate deformation e.g. Richardson [1992]. These forces are the result of lateral variations in density. Any difference in density might arise from changes in crustal thickness or changes in the density of crustal material. Major lateral variations in density (see Figure 2.4.1) occur for example at (a) continental margins, (b) spreading mid-oceanic ridges, and (c) highly elevated regions.

(a) At (passive) continental margins, a significant decrease of topography/bathymetry and crustal thickness towards the oceanic basin are a common result of rifting [Reemst, 1995]. This results in continental crust next to water along the surface (large density difference) and continental crust next to mantle material at deeper levels (small density difference).



Values used to determine TRS

T_i = temperature at base lithosphere	1280 °C
T_s = temperature at surface	0 °C
h_w = waterdepth above MOR	2.5 km
h_b = oceanic crust thickness at MOR	7.0 km
ρ_w = seawater density	1030 kg/m ³
ρ_b = oceanic crust density	2960 kg/m ³
ρ_a = asthenosphere density at T_i	3238 kg/m ³
a_v = coefficient of thermal expansion	$3 \cdot 10^{-5}/K$
z_{iso} = depth of equipotential surface	125 km

Figure 2.4.1

Figure showing four different lithospheric columns in local isostasy that have a potential energy difference with respect to each other. The difference in potential energy between a local lithospheric column and some column defining the reference tectonic state (TRS) is calculated by integration of the vertical stress in a lithospheric column, conform Coblenz et al. [1994]. The difference in potential energy between two columns divided by their distance defines the forces due to lateral density variations. The included table shows values that have been used in this study to determine the Tectonic Reference State.

(b) The spreading of an ocean basin involves uplift of a mid-oceanic ridge at which asthenosphere derived melts well up to the sea floor and upon cooling are accreted as oceanic crust to the diverging plate margins. The young crust is cooling, becomes denser and tends to sink creating abyssal plains, deep oceanic basins [Parsons & Sclater, 1977]. The age-depth relationship of oceanic crust is explained briefly in section 2.3.2 and more detailed in Appendix A. The so-called ridge push force is the (passive) effect of this cooling oceanic lithosphere rather than an active push by up-welling asthenospheric material (see e.g. Bott [1991, 1993] and Ziegler *et al.*, [2001]). The boundary between asthenosphere and lithosphere is defined as temperature dependent, moving away from the ridge, the new-formed material is cooling and, therefore, the lithosphere is thickening. Apart from the density difference between young oceanic

lithosphere and water, the change in lithospheric thickness has a large effect on the density distribution.

(c) In the case of highly elevated regions, kinetic energy that has been used to construct a pile of thrust sheets/crustal thickening is being stored as potential energy in (crustal) topography. Highly elevated regions are most often supported by a crustal root, meaning that at depth light (crustal) material replaces dense (mantle material), while along the surface air is next to dense (crustal) material in a mountain range. The presence or absence of a lithospheric slab under a mountain range will have important effects on potential deviatoric stresses [Bott, 1991].

2.4.1 Concept and calculation

Consider a lithospheric column in isostatic equilibrium (see Figure 2.4.1.1, column 1). The vertical stress in the considered column is given by:

$$\text{Vertical stress} = g[\rho_m (z_{\text{iso}} - z_m) + \rho_c (z_m - h)]$$

where g is the gravitational acceleration, ρ_m and ρ_c are the density of mantle and crust material, z_{iso} is the equipotential level, h is topography, and z_m is the crust-mantle boundary.

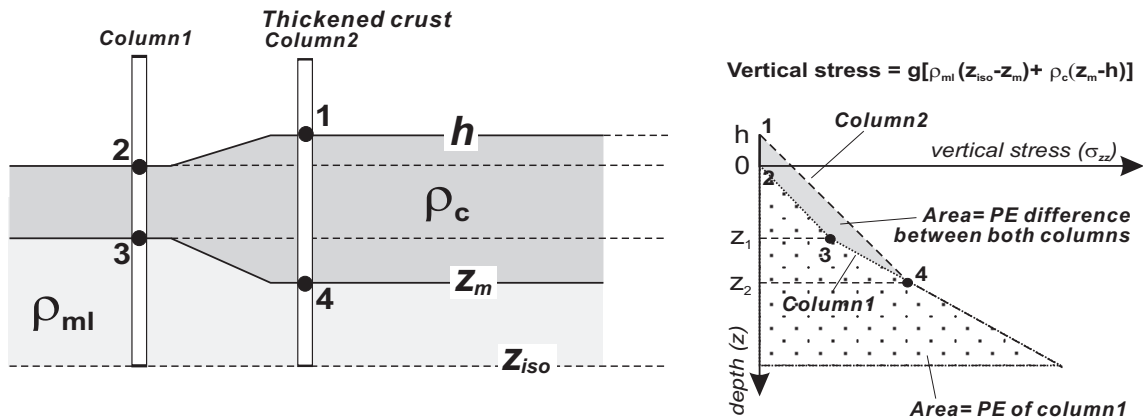


Figure 2.4.1.1

To illustrate the concept of potential energy differences: column 2 has a higher amount of vertical stress than column 1 (gray area below line difference with dotted area) which results in a higher Potential Energy per unit area for column 2. Divided by the distance between both columns, a force pointing down slope would be resulting in tension in the thickened crust and compression in the 'normal' setting.

This vertical stress is through gravity directly related to the amount of material above z_m and the density of this material. The potential energy (per unit area) of the specified column is defined as the integral of the vertical stress in the column. Another lithospheric column that is in isostatic equilibrium as well, but with another density distribution (column 2), might therefore have a different amount of potential energy. Thus, in Figure 2.4.1.1b, the curves denote the vertical stress of two columns and the area below these curves represents the potential energy. Differences in potential energy (shaded area in Figure 2.4.1.1b) are directly related to differences in density distribution between the columns. Divided by the distance between the considered columns, the potential energy becomes a force (per unit area). Obviously, stresses induced by lateral density variations will be largest in areas with large changes in crustal configuration whereas these forces will be oriented perpendicular to the gradient of change.

To evaluate differences in potential energy between areas, a Tectonic Reference State (TRS) has to be defined. This TRS is a column that is supposed to be in isostatic and stress balance with mid-ocean ridges and will not be deformed in the absence of external forces. In other words: in the absence of plate tectonic forces, this is the setting the crust would finally equilibrate to. Different types of TRS have been applied in former studies. [Jones *et al.*, 1996] adopted an asthenospheric column with density ρ_a with its top 2.4km below sea level and no water or lithosphere above it. Based on the mean global potential energy, a column of 30km continental crust (density contrast with mantle of 488 kg/m³) at sea level equivalent to cooling oceanic lithosphere at 4.3km below sea level would represent another useful TRS [Coblentz *et al.*, 1994]. Differences between the alternative reference states would be of the order of 10^{12} N/m [Jones *et al.*, 1998]. TABLE TRS shows the values used to define the TRS in this thesis (equivalent to Coblentz *et al.* [1994]). Another point of reference required for the calculations is an equipotential level at depth. Below this equipotential level, no compensation by density variations is assumed and therefore potential energy differences are absent. After Coblentz *et al.* [1994], who stated that the contribution to potential energy variations from lateral variation of density beneath a depth of 125km is negligible, I adopted an equipotential surface at this depth. This is equivalent to assuming that the thickness of the lithosphere is 125km and the asthenosphere is a homogeneous medium. The potential energy difference of an arbitrary column and the TRS can now be calculated. When the potential energy of the specified column is lower than the TRS, this column should be in deviatoric compression whereas a column with a higher potential energy should be in tension. In the absence of far field forces this would result in extensional forces dominating in thickened crustal regions versus compressional in low lands.

Several authors have successfully applied the concept of stresses induced by lateral density variations to explain regional variations in large-scale (plate-wide) present-day stress fields. Examples are the Indo-Australian plate [Coblentz *et al.*, 1995], the S. American plate [Richardson & Coblentz, 1994]; [Meijer, 1995], the western part of the Eurasian plate [Gölke & Coblentz, 1996], the Philippine plate [Pacanovsky *et al.*, 1999] and the African plate [Coblentz & Sandiford, 1994]. The forces related to potential energy variation can regionally modify the stress field in great detail and change the settings under which a mechanical equilibrium is reached. Crustal thickness variations are important here and can be both the effect of a plate wide stress field, and cause a regional stress field. Two examples are (a) continental margins and (b) active crustal thickening.

(a) Opening of oceans may cause reorganizations of spreading axes. However, in most cases present-day margins will be oriented approximately perpendicular to the ridge push forces because passive margins are the result of crustal separation and ensuing sea-floor spreading. This is for example the case at the Norwegian margin, which is oriented perpendicular to the regional stress field. In this region, the introduction of forces related to lateral density variation (extension parallel to the regional compressive stress field) results in near anisotropic stress circumstances [Gölke *et al.*, 1996].

(b) In a zone of active thickening of continental, the bulk of thickening will occur perpendicular to the Sh_{max} direction, leading to a major gradient in lateral density variations parallel to the regional Sh_{max} direction. Kinetic energy is stored as high levels of potential energy in the thickened region. At a certain moment the extensional forces induced by the increasing difference in potential energy between mountain range and foreland can locally become larger than the compressional forces leading to the deformation (see Figure 2.4.1.2). So, coaxial stress tensors can be expected during tectonic history. Theoretically, this imposes a maximum altitude for thickened continental

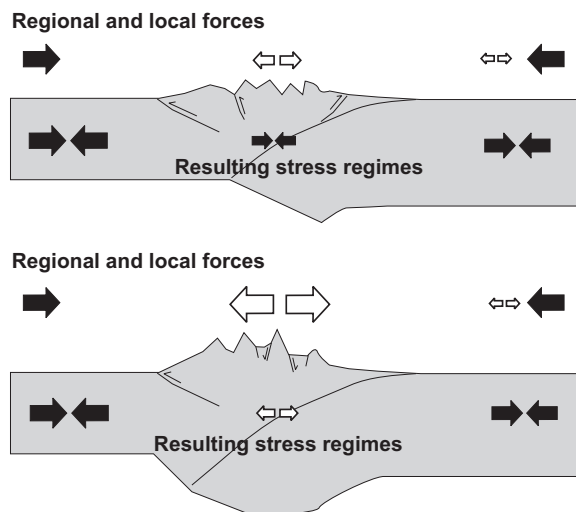


Figure 2.4.1.2

Figure demonstrating how the local stress patterns are combined results of far field stresses and induced dynamic stresses. A mechanical equilibrium is reached for both of the examples. In the lower panel are the induced dynamic tensile stresses larger than the regional compression, resulting in local extension in the mountain range.

crust, based on (1) the magnitude of far field forces and (2) the material the crust is composed of. To what extent extensional features develop or even lead to the 'extensional collapse' of a mountain range (see e.g. [Zhou & Sandiford, 1992]), depends largely on the balance between far-field stresses and the stresses induced by the lateral density variations and therefore reveals information about the magnitude and orientation of the far-field stresses and thus, indirectly about activity of plate boundary processes. Examples of limited extension on top of large actively contracting mountain ranges have been observed in (amongst others) the Andes [Meijer, 1995] and the Himalayan belt [Colchen, 1999] and have been observed for the tectonic evolution of the Alpine range as well (Gosau basins [Willingshofer, 2000]). Complete extensional collapse due to high levels of

potential energy stored in zones of thickened crust can occur when the far-field stresses responsible for the build up of the orogenically thickened zone diminish by a decrease in convergence rate, rotation of the main compression direction or slab break off [Bott, 1993]. This concept has been proposed as 'extensional collapse' for amongst others, the Betic and Alboran region [Vissers *et al.*, 1995]. Jones *et al.* [1998] linked potential energy driven extension of the Laramide orogeny (North America) to paleo-elevations of the region and calculated that elevations required for extensional collapse to occur would have had to reach over 3500m. Bada [1999] was the first to incorporate estimates of reconstructed crustal thickening in the geological past in numerical modelling of paleostress fields of the Pannonian Basin (see also Bada *et al.* [2001]). By comparison of modelling results with careful reconstruction of the paleostress field, these authors were able to estimate minimal crustal thickness in the Eastern Alps that would be required for extensional collapse of this region.

The main uncertainties in the potential energy calculations are related to:

(1) Density distribution. Especially in continental crust, which is far from homogeneous, this is a major uncertainty. If crust in a region consists of very dense material, whereas average density of continental density is used in the calculations, this will lead to an underestimation of the stresses induced by the structure.

(2) Geometry of crustal thickness (Moho topography). Indirect methods for observing the transition from crust to mantle (seismic refraction and reflection) have only covered a limited extent of the world yet. In general, across mountain ranges quite a number of very well controlled geotransects have imaged the Moho very well. However, its continuation in any direction is not well resolved.

(3) The influence of lithosphere thickness variations and the choice of an equipotential surface at depth. Although the density difference between asthenosphere and lithosphere is relatively small, the large volumes considered might have significant influence. In case the lower crust is decoupling the upper crust from the mantle, the forces that are related to this lithosphere topography would only have a very limited

effect on the crustal state of stress. First order estimates from studies of large scale lithospheric stress induced by global mantle circulation [Steinberger *et al.*, 1999] show that non-hydrostatic lithospheric stress might vary between -140 and 140 MPa. For the Iberian Peninsula values only range from $+40$ to 0 MPa.

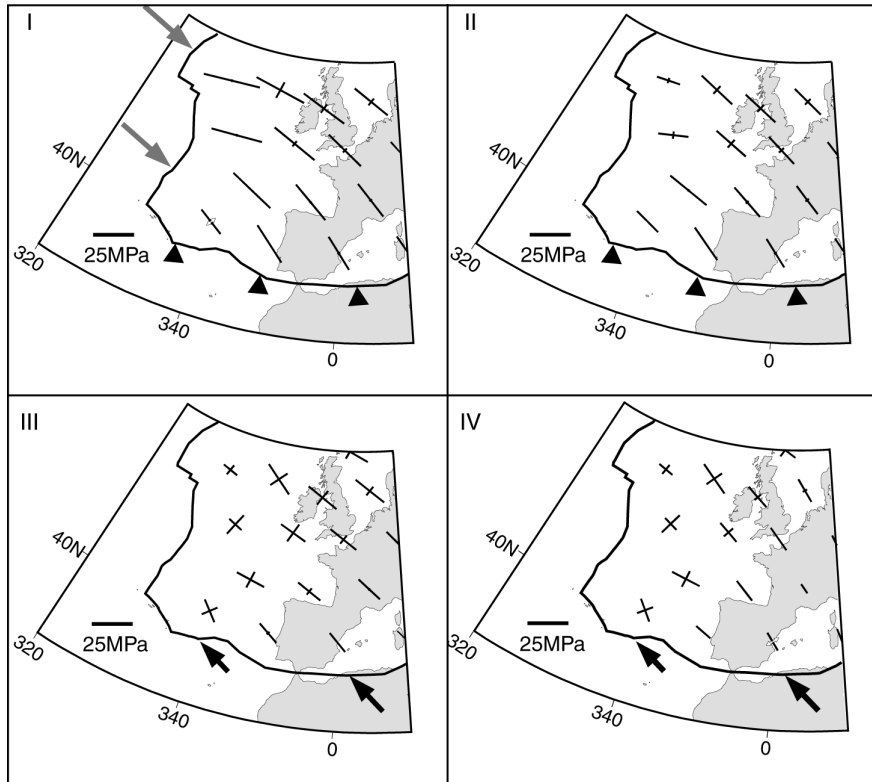


Figure 2.4.1.3
Predictions from numerical modelling of the stress field of western Europe after Gölke and Coblenz [1996]; model results for a reference thickness of 100km using a uniform elastic rheology. The panels display the predicted stress patterns for in Iberia and surrounding areas for different models. See reference and text for more detailed description.

The effect of stresses induced by lateral density variations is expected to be significant for the Iberian Peninsula as suggested by (a) large scale modelling of the European plate by Gölke *et al.* [1996], (b) crustal configuration in the region, and (c) seismic activity in NW Iberia, far from any active plate boundary. To motivate (a), note that finite element models on the stress field for the shelf of mid-Norway [Gölke *et al.*, 1996] show second order tensile stresses that are large enough to create a local stress state with a small stress anisotropy. This means that the horizontal principal stresses are about equal in magnitude, which enables permutation of the maximum and intermediate principal axes. It should be noted that along the Norwegian margin, the decrease in thickness of the continental crust and the far field maximum horizontal compression are parallel. Therefore, the induced extensional forces counteract the regional compression. A large step in topography and crustal thicknesses along the western and northern coast of Iberia, similar to the mid-Norwegian shelf, causes potential energy driven tensional stresses in the same order of magnitude (about 15MPa, [Gölke & Coblenz, 1996]) as for the Norwegian margin. Results of Gölke & Coblenz [1996] show that if stresses generated by distributed ridge push and buoyancy forces are incorporated, the orientation of Sh_{max} does not change significantly for continental Iberia with respect to the model without buoyancy forces (see Figure 2.4.1.3). The local state of stress in Iberia (ratio between the principal stress-axes), however, is altered very much as well by both reduction of the Sh_{max} magnitude (see Figure 2.4.1.3, panel I versus panel IV) as well as by increasing importance of the other principal stresses (uniaxial compression

versus strike-slip regime). For the oceanic part, it is clear that incorporation of these forces (compare Figure 2.4.1.3 panel II with panel III and IV) leads to a dramatic change in stress field orientation and magnitude. (b) Since convergence between Africa and Eurasia started in the Campanian (see Chapter 4 for detailed outline), Iberia was progressively subjected to compressional stresses between both plates. Additional compression from the west, related to ridge push forces of the Mid Atlantic Ridge, hindered lateral escape to the west and even added to high levels of intraplate stress. Stress was released by internal deformation: the Iberian Peninsula shows significant internal deformation, has a thickened crust (average at about 30-35 km), relatively elevated average topography (400 m, [Stapel, 1999]), and shows evidence for folding at lithospheric scale [Cloetingh *et al.*, 2001]. Along the northern and western margins of Iberia steep gradients in crustal thickness changes occur. (c) Most seismicity in Iberia (see Figure 2.4.1.4) can be related to active plate boundaries (Mid Ocean Ridge, Azores, African-Eurasian boundary) or weak zones related to former active plate boundaries (Pyrenees/Betics). However, from November 1996 until May 1997 an area of approximately 20km² near Lugo, located in Galicia (NW Iberia) was struck by over 250 seismic events ranging in magnitudes from 3.0 to 5.1 (Mb). Whereas these magnitudes are relatively low, the seismic activity in this region is remarkable when taking into account the large distance to any of the active plate boundaries. Focal mechanism solutions of this pronounced seismic activity indicate active normal faulting along roughly N-S trending faults ([SIGMA, 1998] and online databases Instituto Geográfico Nacional, <http://www.geo.ign.es> or Harvard CMT Catalog, <http://www.seismology.harvard.edu/CMTsearch.html>). The orientation of the regional present-day compressional stress is at large angles to the western and northern margins. An additional source of sub-parallel extensional stresses related to lateral density variations along both margins could modify the local state of stress in such a way that normal motion of the N-S oriented faults can be explained. In this respect it is remarkable that the concentration of seismicity occurred at the cross point of (weak) seismic alignments along the northern and western coast. To test this hypothesis on the occurrence of the seismicity in northwestern Iberia and to enable a better estimate of the local state of stress for regions in Iberia, the concept of lateral density variations has been incorporated in the modelling. Combined with local information on the crustal configuration (pre-existing faults, weakness zones), the proximity to failure of the crust can be evaluated, enabling a more accurate evaluation of seismic hazard.

2.4.2 Testing the model-sensitivity for various input parameters

This section presents the effects of a more data-oriented approach by (a) a comparison between the effect of using filtered observed bathymetry of the ocean floor off shore Iberia or using the theoretical age-dependence curve, and (b) the effect of sampling independent data on crustal thickness from Bouguer inversion instead of using the concept of local isostasy to calculate the crustal thickness as a function of surface topography. Especially the data used as input and the methods to define crustal configuration of the concept could have important effect on the magnitudes of the induced stresses [Andeweg *et al.*, 1999b]. E.g., in previous work by Coblenz *et al.* [1994] and Meijer [1995], the theoretical age-dependent depth of the oceanic crust has been used, in combination with a crustal thickness derived from sampled topography combined with the concept of isostasy.

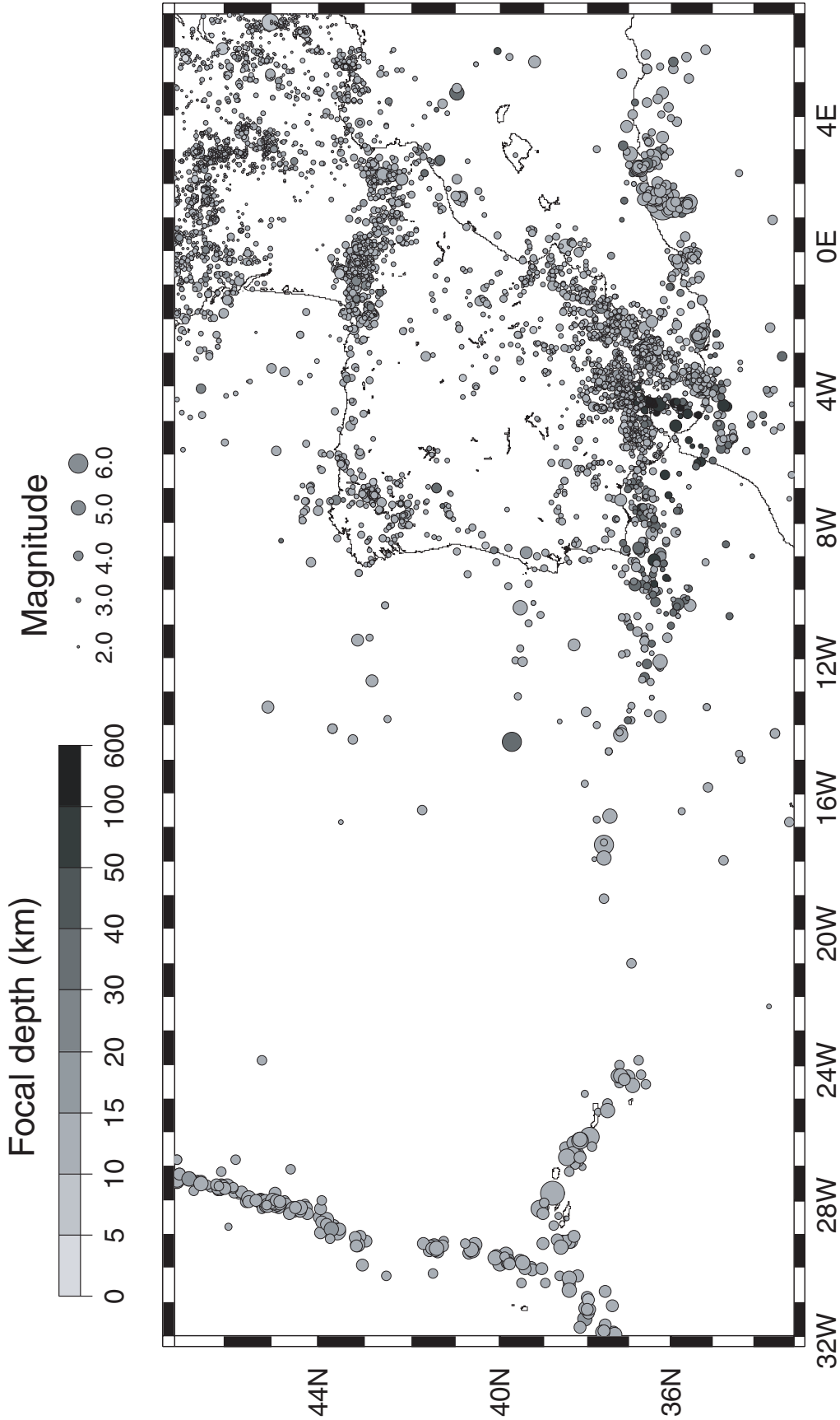


Figure 2.4.1.4
 Map showing distribution, magnitude and focal depth of earthquakes from 1980-1996. Based on data by SIGMA [1998] and online databases Instituto Geográfico Nacional, (<http://www.geo.ign.es>) or Harvard CMT Catalog (<http://www.seismology.harvard.edu/CMTsearch.html>). Major part of the seismic activity is related to active and former plate boundaries (Mid Ocean Ridge, Northern Africa and Pyrenees, Betics respectively).

(a) Bathymetry

The above-cited references use the theoretical age-dependent curve to determine the bathymetry of the ocean floor. After sampling the age of oceanic crust from a global ocean floor age database [Mueller *et al.*, 1995], the depth of oceanic seabed (d) has been calculated according to the theoretical age-depth $d(t)$ curves by Parsons & Sclater [1977]

$$d(t) = 2500 + 350 \sqrt{t}$$

for oceanic lithosphere younger than 70Ma, and

$$d(t) = 6400 - 3200 (-t/62.8)$$

for older ocean floor. Subsequently, this theoretical bathymetry is used in the potential energy calculations. The limit between old and young oceanic lithosphere has been chosen as the 70 Ma isochron, coinciding with the change from one formula to the other.

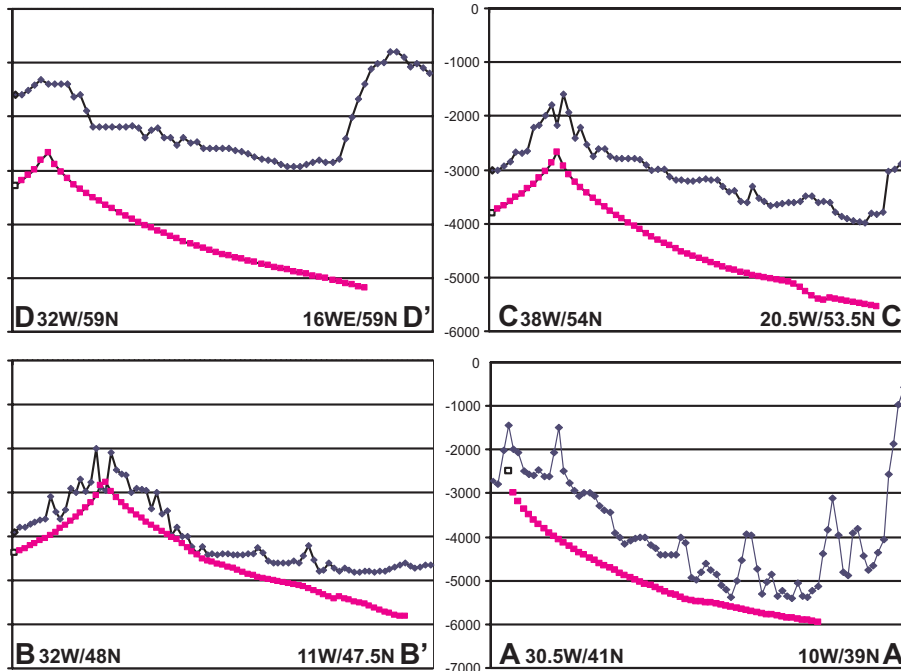
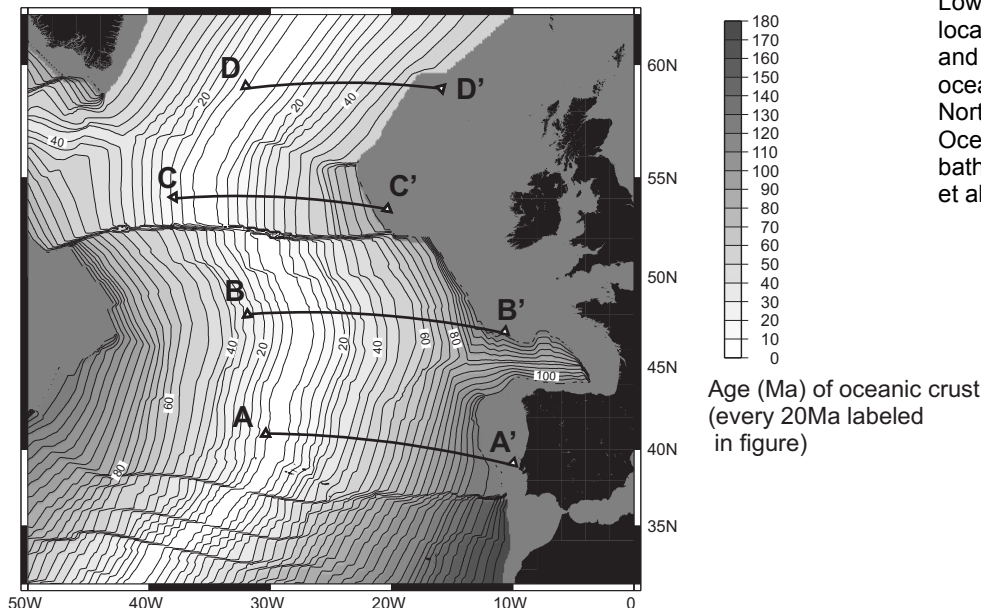


Figure 2.4.2.1
Four bathymetric profiles from the Mid Atlantic Ridge to the east show a large difference between observed depth (black dots) of oceanic crust (upgoing curves to the right due to arrival at the continental margin) and the theoretical curves (gray dots) as calculated using the age-depth relations by Parson & Sclater [1977]. Only for profile B-B' the fit is acceptable. In the other profiles a difference of over 1000 m is normal. Lower panel shows location of profiles and age of the oceanic crust in the Northern Atlantic Ocean. Source of bathymetry: Müller *et al.* [1995].



Applying the theoretical curve, the mid-ocean ridge (where age of the crust is 0 Ma) would be at 2500m below water surface.

In the case of the eastern North Atlantic however, the ridge deviates significantly from this theoretical depth. At the Azores triple point, the Mid Atlantic Ridge reaches up to 1400m under the water surface, further north the ridge shallows progressively to reach the surface at Iceland. It has been known that this curve almost always predicts too-deep depths for old ages as well [Stein & Stein, 1992] Furthermore, parts of the oceanic basin have been deformed during the Tertiary, for example Kings Trough. Figure 2.4.2.1 shows four profiles running from the Mid Atlantic Ridge to the coast of Western Europe. Note the large difference between the observed and theoretical curves for all of the profiles, in extreme for the northernmost profile (more than 2000m difference). These differences have an important influence on the magnitudes of the ridge push forces.

(b) Crustal thickness

In order to calculate crustal thickness according to the approach of Coblenz *et al.* [1994] the topography of continents has been sampled from topographic databases (e.g. ETOPO5, [NOAA, 1988]) and has been filtered with a low-pass filter taking a boundary wavelength of 100km, simulating regional isostasy. This approach will eliminate local effects and topographic features related to small-scale stress sources (e.g. flexure). Then, using the concept of isostasy and reference densities of 2700kg/m^3 for crust and 3300kg/m^3 for mantle, two slightly different equations (see appendix of Coblenz *et al.* [1994]) are used to deduce crustal thickness for continental margin (thinned continental) and elevated continental settings, respectively. Shore-line is the separator between thinned continent and elevated continent.

An alternative approach to obtain information on crustal thickness would be sampling independent data, as for example gravity or deep seismic data. The best method would be to use direct observations from seismic determinations of Moho depth. Although over the last decades the number of seismic data points for Iberia has been increasing (e.g. Pulgar *et al.* [1997]; Jabaloy *et al.* [1995]), data coverage is still limited and distributed inhomogeneously. To construct a grid of Moho depths from these values would likely introduce large errors. Another method is using gravity data, which are available for the entire Iberian Peninsula. The distribution of dense or light material in the crust is reflected in its gravity signal. The free air anomaly is the deviation from the geoid, while the Bouguer anomaly reflects changes in density at depth since it is obtained by correcting the Free-air gravity anomaly for topography and bathymetry. Assuming a reference density for the continental crust and a reference depth, Bouguer data can be inverted to obtain an approximation of crustal thickness, for Iberia performed by Stapel [1999]. The method is internally consistent with the isostatic calculations because reference density and depth (2700kg/m^3 and 30km, respectively) are equal to those applied to determine the TRS (see Figure 2.4.1).

In case of plate-wide models with elements covering hundreds of kilometers, the use of a reference density and local isostasy seems valid. A study of isostatic residuals by Stapel [1999] shows that in major part of Iberia the isostatic residuals are not zero, which indicates that topographic loads and buoyancy forces are not in balance. As a result of this, crustal thickness is over- or underestimated (excess or deficient topography for the crustal thickness and the used reference density). One way to explain the complicated isostatic residuals are dynamic forces acting on the lithosphere as for example plate boundary forces or forces generated by convection in the mantle. One should keep in mind that for the determination of the isostatic residual a reference density is used, so variations in density could explain some of the misfit.

Especially for regions that are far from local isostasy (high isostatic residuals) crustal thicknesses differ significantly, which will have large effects on the calculated stresses induced by lateral density variations.

Testing scenarios

Figure 2.4.2.2 shows a flow chart of the modelling procedure, from construction of a model through the calculation of the forces induced by lateral density variations. The ANSYS © finite element package was used to create the model and calculate the resulting stress field. Potential energy per node was calculated using 'Potenca' (Andeweg, not published), a modification of the potential energy calculation program by Coblenz *et al.* [1994]. Several routines (A2P and P2A, Andeweg, not published) have been developed to communicate between ANSYS and Potenca.

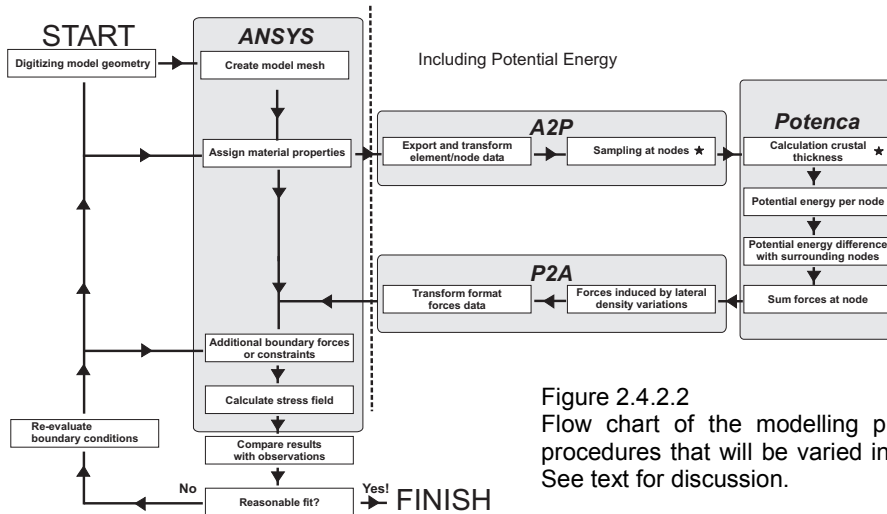


Figure 2.4.2.2
Flow chart of the modelling procedure. Stars denote procedures that will be varied in the different scenarios. See text for discussion.

To demonstrate the effect of the different approaches on the induced forces, the input data resulting from these will be used in the potential energy calculations is presented for an area of 27 x 7 degrees (see Figure 2.4.2.3), elongated perpendicular to the margin of NW Iberia. The area is chosen to include young and old oceanic crust, continental margin, and elevated continent. For all scenarios, the area has been meshed in the same way with elements with a typical side length of about 50km. In order to obtain realistic magnitudes of forces and thus to be able to evaluate the resulting differences with respect to observations, the scenarios have been tested on a model for the European plate (further details are described in Chapter 6). A realistic collision force (see Chapter 6) has been applied along the southern boundary (African-European collision) to be able to directly compare the effect of the induced forces on effective stress levels, on the state of stress and the orientation of the principal stress axes in the Iberian Peninsula.

Scenario Ia (Coblentz)

Rationale: standard method used by previous studies based on Coblenz *et al.* [1994].

Description: bathymetry calculated as theoretical ocean floor depth and crustal thickness calculated from filtered topography (wavelength of 100 km) using local isostasy.

Results: Using the theoretical ocean floor depth to calculate the induced forces yields a rather smooth pattern of ridge push forces towards the continent. This is not a surprise, since the theoretical curve deepens gradually. The steep continental margin induces important forces pointing in the opposite direction. Integrated, these forces are of lesser importance than the ridge push forces, but their local effect on stress magnitude and

state of stress is significant (note strong decrease of maximum horizontal compression along the northern and western margins of Iberia, see Figure 2.4.2.4). The resulting pattern of local stress states fits very well to the observations. Effective stress magnitudes (the difference between the principal stress axes) in Iberia are modelled to be of the order of ~ 25 MPa.

Scenario Ib (Ridge close to sea-level)

Rationale: in reality the Mid Atlantic Ridge is closer to sea level than the theoretical value of 2500m.

Description: bathymetry calculated as theoretical ocean floor depth but starting from a ridge at 1425m instead of 2500m, for the rest of the setting equal to scenario I.

Results: the curvature of the mid-oceanic ridge is similar to that in scenario Ia, but the ridge is closer to sea level. This results in a larger difference with the defined Tectonic Reference State than in scenario 1a. Therefore, the associated ridge push forces are larger, which decreases the effect of the stresses induced by the margin or on-shore crustal topography. To obtain a reasonable resemblance with the directions of the observed stress field, the collision forces along the southern boundary have to be increased by over 100% resulting in relatively high stress levels in the Iberian Peninsula of over 80MPa.

Scenario II (Real bathymetry)

Rationale: the ocean floor offshore Iberia shows large-scale irregularities that differ significantly from the theoretical age-depth curve.

Description: bathymetry and topography sampled from ETOPO5 database and filtered with a low-pass filter applying a boundary wavelength of 100 km, crustal thickness calculated using local isostasy and the filtered values for bathymetry/topography.

Results: the complex physiography of the ocean floor (e.g. Kings Trough and Gorringer Bank) distorts the smooth pattern of forces acting towards the continent. Large forces are related to these features and due to their intermediate position between ridge and continent, the forces counteract each other to large extent. Subsequently, less integrated ridge push force is transmitted to the continent (see Figure 2.4.2.5) than for the previous scenario. Although the directions of the observed and modelled trajectories yield the best fit using this approach, only limited levels of resulting effective stress (on average ~ 15 MPa) are being reproduced for the Iberian Peninsula. These relatively low magnitudes for the effective stress would most probably not be able to account for the observed deformation.

Scenario III (Inverted Moho)

Rationale: calculating crustal thickness from topography using local isostasy implies a very important but uncertain assumption (see above). Using independent data on crustal thickness would be a more correct approach.

Description: topography and bathymetry sampled from ETOPO5 and filtered with low-pass filter applying a boundary wavelength of 100 km, Moho-depth sampled from Bouguer anomaly inversion (during this testing only available for region 16W/1E/35S/45N).

Results: higher levels of compression enter the Iberian mainland (effective stresses ~ 50 MPa), stresses concentrate along the a-typical margins of the Iberian Peninsula (up to more than 100MPa), see Figure 2.4.2.6. The latter is the result of the presence of local bathymetrical highs (amongst others Gorringer Bank, Galicia Bank, Vigo Seamount) that show important isostatic residuals [Stapel, 1999], in other words are not supported by thickened crust. Regions with a large isostatic residual have a strong influence on the

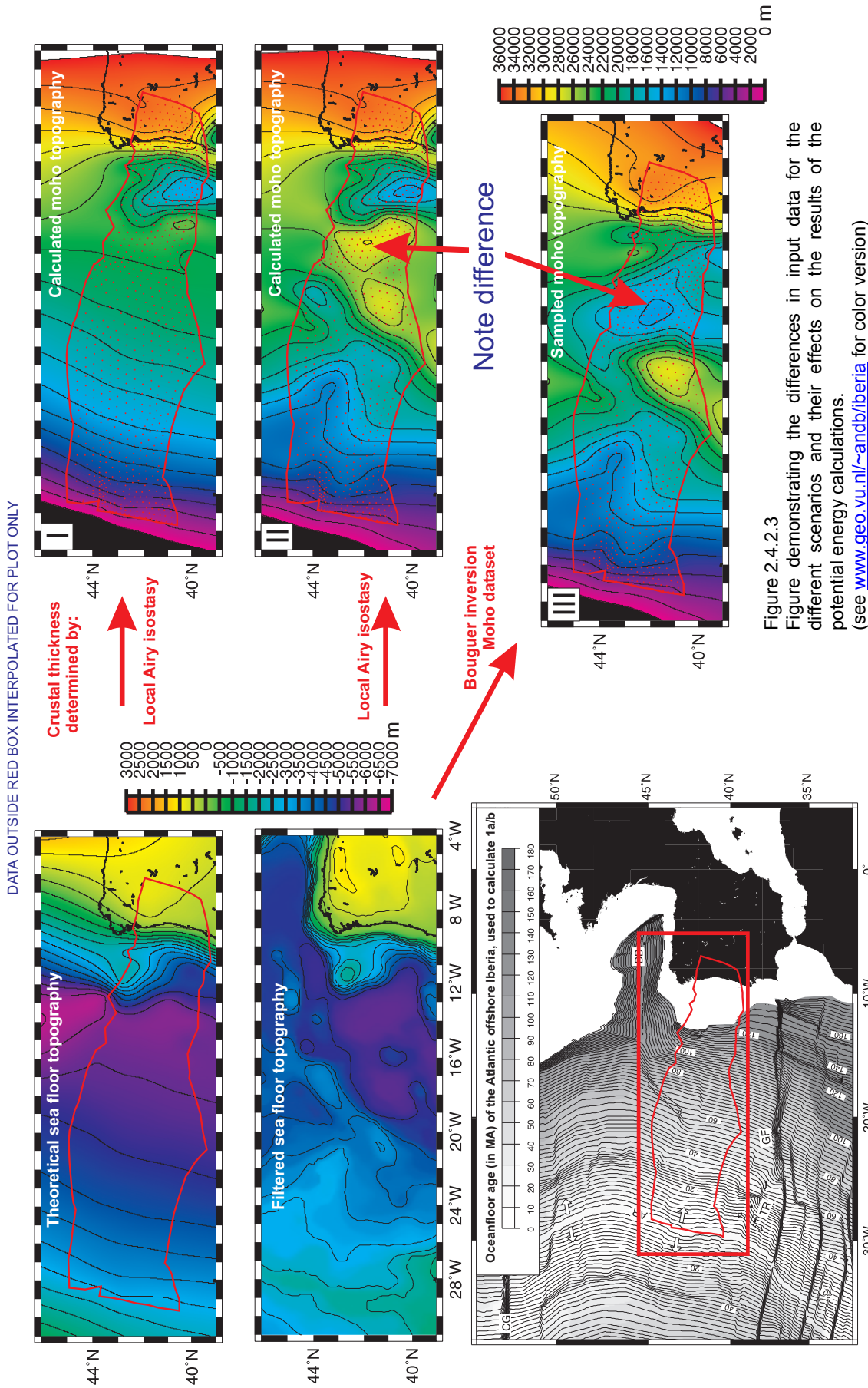


Figure 2.4.2.3
Figure demonstrating the differences in input data for the different scenarios and their effects on the results of the potential energy calculations.
(see www.geo.vu.nl/~andb/iberia for color version)

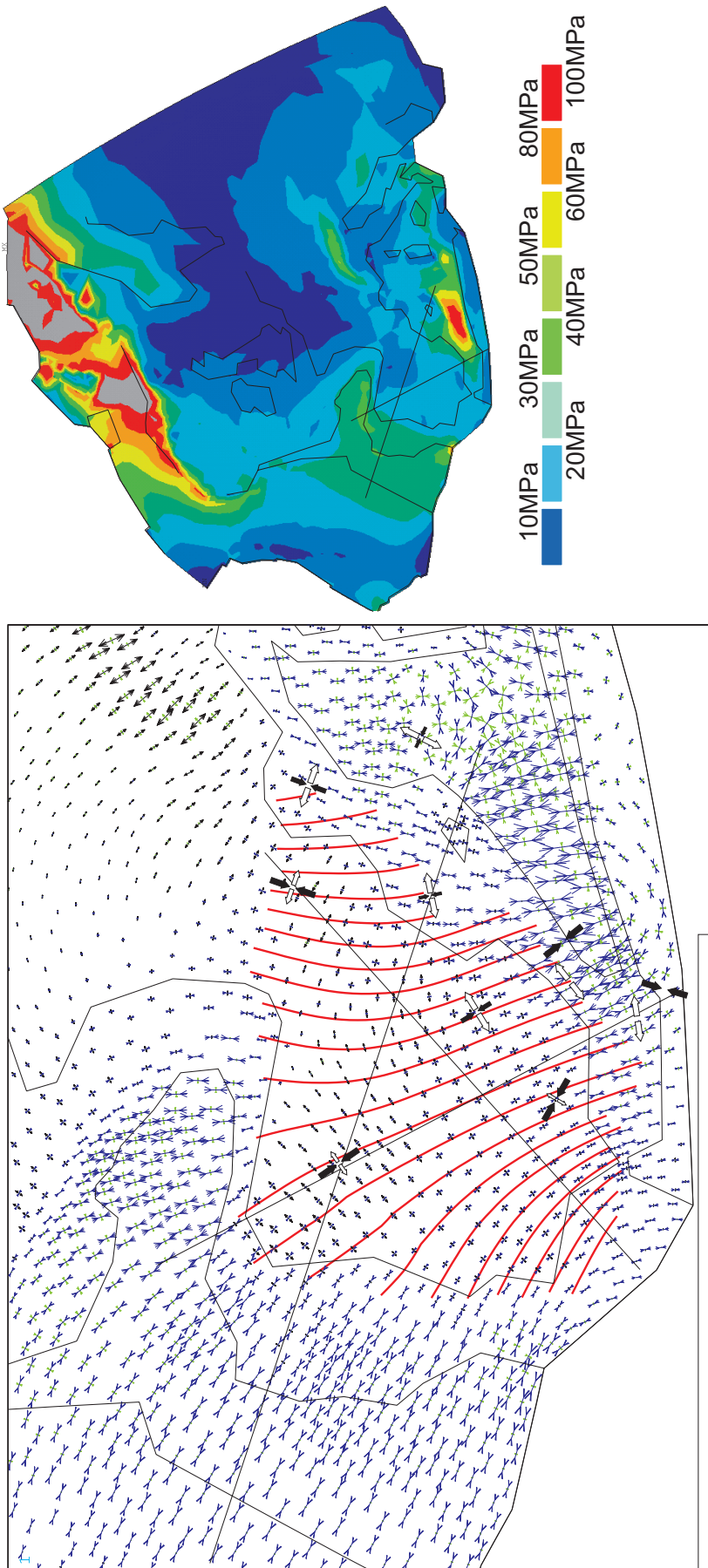


Figure 2.4.2.4
 Model result for scenario I, including a modified theoretical bathymetry and an “isostatic” topography.
 Left panel: predicted patterns for principal axes of stress for Iberia and surrounding region.
 Right panel: predicted levels of effective stress in western Europe.
 (see www.geo.vu.nl/~andb/iberia for color version)

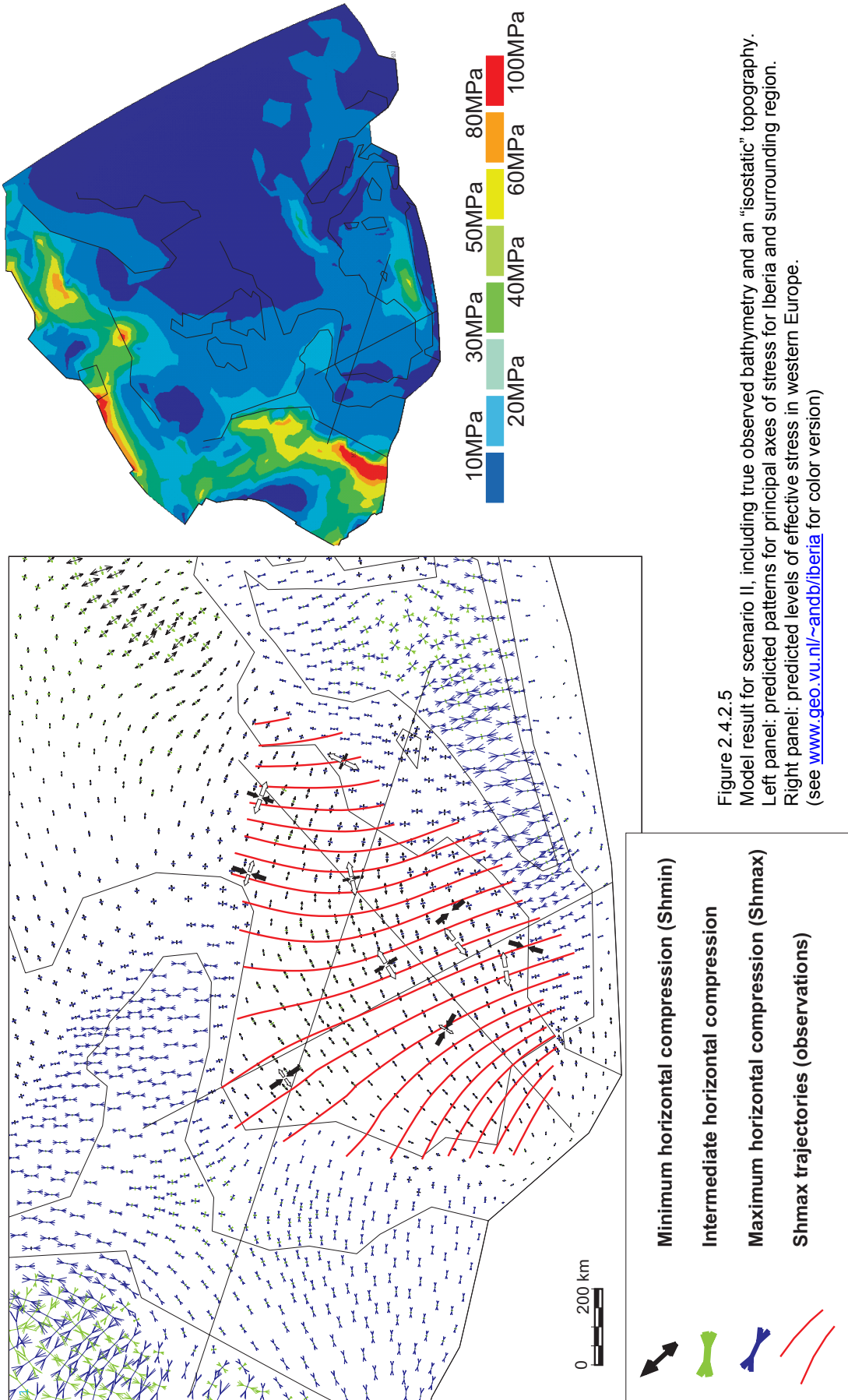


Figure 2.4.2.5
 Model result for scenario II, including true observed bathymetry and an “isostatic” topography.
 Left panel: predicted patterns for principal axes of stress for Iberia and surrounding region.
 Right panel: predicted levels of effective stress in western Europe.
 (see www.geo.vu.nl/~andb/iberia for color version)

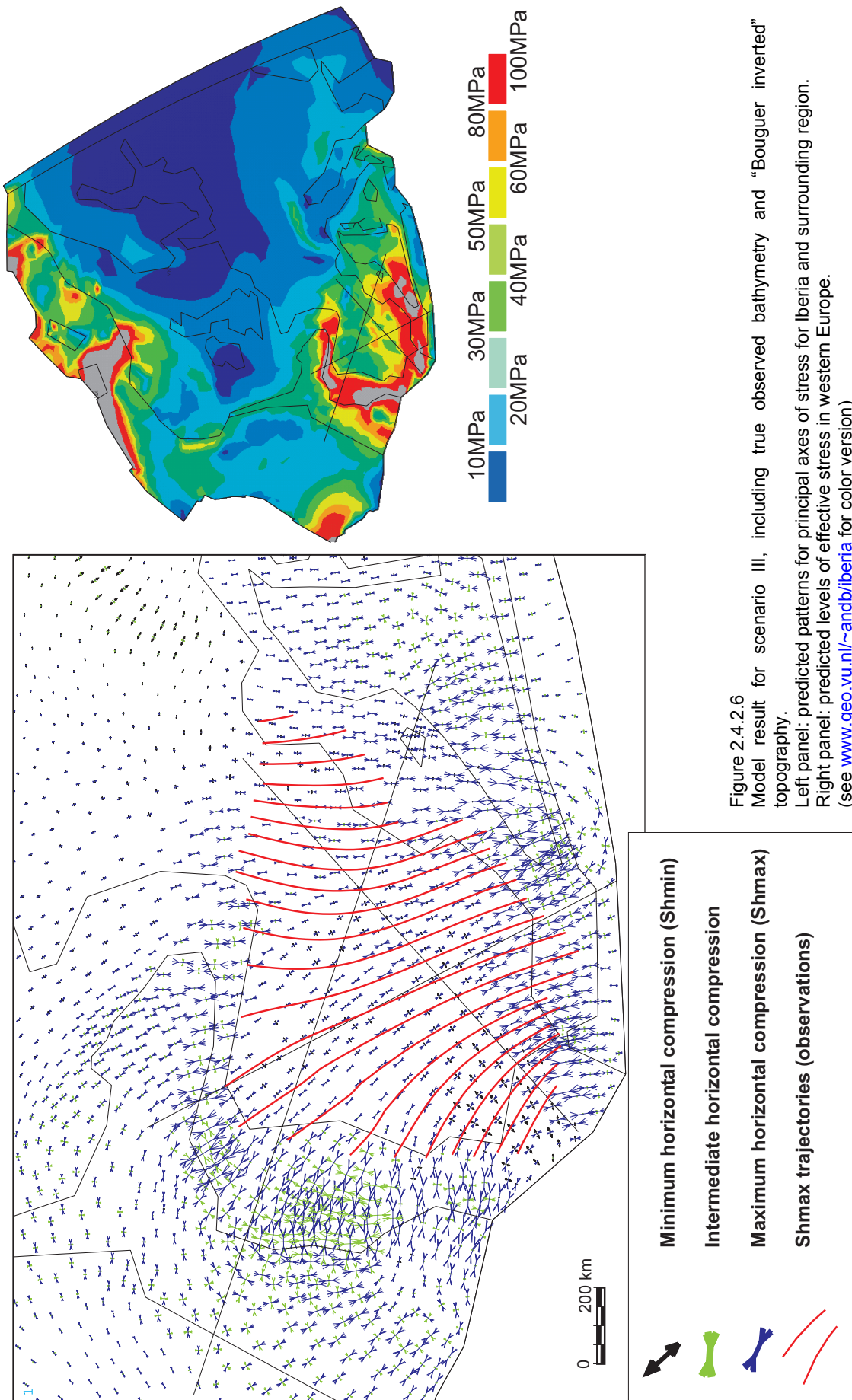


Figure 2.4.2.6

Model result for scenario III, including true observed bathymetry and “Bouguer inverted” topography.

Left panel: predicted patterns for principal axes of stress for Iberia and surrounding region.

Right panel: predicted levels of effective stress in western Europe. (see www.geo.vu.nl/~andb/iberia/ for color version)

induced forces. In case of Gorringe Bank, the presence of dynamic forces uplifting the shallow oceanic crust are inferred [Souriau, 1984], which can be easily related to the present-day active plate boundary.

This inversion of Bouguer data to obtain Moho depth shows huge misfits with the restricted amount of seismic observations of the Moho in the Alpine regions Iberia and the North Atlantic [Stapel, 1999]. For the strongly deformed areas a possible explanation is given: the method of Bouguer inversion can only produce smooth surfaces, while large scale offsets of the Moho have been observed (e.g. line ESCIBETICAS-1 [Jabaloy *et al.*, 1995] and ESCI-N2 [Pulgar *et al.*, 1997]). An additional reason for the misfit is the large deviations from assuming a reference depth of 30km and an average density for continental crust in Alpine deformed regions. The same pattern of fit and misfit is observed between the calculated Moho depth using filtered present-day topography and the concept of local isostasy and the Bouguer inverted Moho database. Fit is rather good in the central parts of Iberia, but misfits occur in the deformed regions and offshore.

2.4.3 General model results and conclusions:

In general the orientation of $S_{h_{max}}$ shows a rather good fit for all three approaches. The pattern of the state of stress and the levels of effective stress, however, show large differences, due to the varying magnitudes of the stress component induced by the lateral variations in gravitational potential energy for the various scenarios. When compared with observations of the present-day stress field in the Iberian Peninsula, the results obtained applying scenario I are best with regard to the local state of stress, whereas, with scenario II the best fit is obtained for the stress trajectories. The effective stress levels predicted by the various scenarios differ quite significantly in magnitude as well. Estimates of intraplate stress levels in France range between 70 ± 15 MPa close to the Pyrenean front to a nearly constant 40 ± 15 MPa [Rocher *et al.*, 2000]. Compared with these levels of intraplate stress, scenario III predicts the best fit. The Mid-Atlantic Ridge and ocean floor offshore Iberian differ significantly from the theoretical curve based on cooling oceanic lithosphere. The western and northern Iberian margins have experienced moderate to intense Alpine deformation due to the opening and closure of the Kings Trough/Bay of Biscay/Pyrenean plate boundary. Large seamounts associated with large gravity anomalies line up along the western and northern margin. The crustal configuration differs significantly depending on the approach applied to determine crustal thickness. Principally, if independent direct observations of crustal thickness are available for the region (e.g. deep seismic profiling) this should be incorporated. However, as long as the knowledge of local density structure is not accurate and reference densities will be used in the calculations, the use of such a database of crustal thickness does not improve the results. While eliminating one error (calculation of crustal thickness based on isostasy), it introduces another due to the lack of information on the crustal density distribution. The same is valid for using inverted gravity data, for which a reference density has to be chosen as well. In plate wide models with large elements, the application of a reference density for crust is more justified than for the smaller element sizes used in this study.

As shown in this Chapter, the orientations of the principal axes of stress are within close range for each of the scenarios. As long as the data on crustal thickness and density distribution are not accurate enough to apply the theoretically more correct scenarios II and III, the use of the internally more consistent scenario of Coblenz *et al.* [1994] as used by the references cited is justified. Due to the incompleteness of the input data set, even more so for the geological past, the first scenario has been used in Chapter 6.